

Higher-Loop Calculations of the Ultraviolet to Infrared Evolution of a Vectorial Gauge Theory in the Limit $N_c \rightarrow \infty$, $N_f \rightarrow \infty$ with N_f/N_c Fixed

Robert Shrock

C. N. Yang Institute for Theoretical Physics, Stony Brook University, Stony Brook, NY 11794

We consider an asymptotically free vectorial $SU(N_c)$ gauge theory with N_f fermions in the fundamental representation and analyze higher-loop contributions to the evolution of the theory from the ultraviolet to the infrared in the limit where $N_c \rightarrow \infty$ and $N_f \rightarrow \infty$ with $r = N_f/N_c$ a fixed, finite constant. We focus on the case where the n -loop beta function has an infrared zero, at $\xi = \xi_{IR,n\ell}$, where $\xi = \alpha N_c$. We give results on $\xi_{IR,n\ell}$, the anomalous dimension of the fermion bilinear evaluated at $\xi_{IR,n\ell}$, denoted $\gamma_{IR,n\ell}$, and certain structural properties of the beta function, β_ξ . The approach to this limit is investigated, and it is shown that the leading correction terms are strongly suppressed, by the factor $1/N_c^2$. This provides an understanding of a type of approximate universality in calculations for moderate values of N_c and N_f , namely that $\alpha_{IR,n\ell}N_c$, $\gamma_{IR,n\ell}$, and structural properties of the beta function are similar in theories with different values of N_c and N_f provided that they have similar values of N_f/N_c . We give results up to four loops for nonsupersymmetric theories and up to three loops for supersymmetric theories.

PACS numbers: 11.15.-q, 11.10.Hi, 11.15.Pg

I. INTRODUCTION

The evolution of an asymptotically free gauge theory from the ultraviolet (UV) to the infrared (IR) is of fundamental field-theoretic interest. The UV to IR evolution of the gauge coupling $g(\mu)$ as a function of the Euclidean momentum scale, μ , is determined by the β function [1]

$$\beta_\alpha \equiv \frac{d\alpha}{dt}, \quad (1.1)$$

where $t = \ln \mu$ and $\alpha(\mu) = g(\mu)^2/(4\pi)$. Here we consider this evolution for a vectorial gauge theory with gauge group $G = SU(N_c)$ and N_f massless fermions ψ_j , $j = 1, \dots, N_f$, transforming according to the fundamental representation of G [2]. We also point out some contrasts with results for fermions in higher-dimensional representations. We focus on the case where the n -loop β function has an infrared zero, at a value $\alpha = \alpha_{IR,n\ell}$. The condition of asymptotic freedom requires that N_f be bounded above by a value $N_{f,b1z}$ where the one-loop coefficient in β vanishes [3]. For large enough N_f (less than $N_{f,b1z}$), the two-loop β function has an infrared zero at a certain value of α , denoted $\alpha_{IR,2\ell}$ [4, 5]. The desire to understand better both the behavior of the running coupling in quantum chromodynamics (QCD) and the properties of an IR zero that occurs for sufficiently large N_f have motivated calculations of higher-loop terms in β [6, 7] and higher-loop corrections to the two-loop result for the IR zero [8]-[12]. In [9, 10], calculations of the IR zero in β , and the associated anomalous dimension of the (gauge-invariant) fermion bilinear, γ_m , were done to four-loop order for an asymptotically free vectorial gauge theory with gauge group G and N_f fermions in an arbitrary representation R , with explicit results for R equal to the fundamental, adjoint, and symmetric and antisymmetric rank-2 tensor representations. Further generalizations and results on higher-loop structural properties of the β function were given in [12].

An interesting and important property that one notices in these calculations for an $SU(N_c)$ theory with N_f massless fermions in the fundamental representation is that the values of the n -loop γ_m , evaluated at $\alpha_{IR,n\ell}$, denoted $\gamma_{IR,n\ell}$, and of the product $\alpha_{IR,n\ell}N_c$, are similar for theories with different values of N_c and N_f , provided that these theories have similar values of the ratio N_f/N_c . Indeed, the computations in [12] show that this is also true for other structural quantities describing the UV to IR evolution, including the derivative of the n -loop beta function, $d\beta_{n\ell}/d\alpha$ evaluated at $\alpha_{IR,n\ell}$ and the products $\alpha_{m,n\ell}N_c$ and $(\beta_{n\ell})_{min}N_c$, where $\alpha_{m,n\ell}$ denotes the value of α where $\beta_{n\ell}$ is a minimum, and $(\beta_{n\ell})_{min}$ is the value of $\beta_{n\ell}$ at this minimum. These observations show that there is an underlying approximate universality in the form of the quantities that control the UV to IR evolution of these theories. This motivates a more detailed study to elucidate this phenomenon. We carry out this study in the present work.

For this purpose, we analyze these theories in the 't Hooft - Veneziano limit [13, 14]

$$N_c \rightarrow \infty, \quad N_f \rightarrow \infty$$

$$\text{with } r \equiv \frac{N_f}{N_c} = \kappa \quad \text{and} \quad \xi(\mu) \equiv \alpha(\mu)N_c = \lambda(\mu), \quad (1.2)$$

where κ is a constant and λ is a function depending only on μ . We will use the symbol \lim_{LNN} for this limit, where “LNN” stands for “large N_c and N_f ” (with the constraints in Eq. (1.2) imposed). The reasons for these two constraints in Eq. (1.2) (that the ratio N_f/N_c and the product $\alpha(\mu)N_c$ are fixed and finite) are that these constitute the necessary and sufficient conditions in order that (i) fermions give nonvanishing contributions to the β function, anomalous dimension γ_m , and other quantities, and (ii) scattering amplitudes remain finite, in the limit

$N_c \rightarrow \infty$, respectively. More generally, if the fermions are nonsinglets under other gauge groups with squared couplings α_i , one also requires that the products $\alpha_i N_c$ be finite as $N_c \rightarrow \infty$ [15].

As we will show in detail below, a study of the LNN limit (1.2) and the approach to it provides an explanation of the approximate universality in the UV to IR evolution of theories with different values of N_c and N_f but the same, or similar, values of r that is exhibited in explicit calculations (with appropriate scalings understood for certain quantities, such as multiplying $\alpha_{IR,n\ell}$ by N_c). A crucial property of the LNN limit is that it reduces the number of variables on which the UV to IR evolution depends. Thus, for finite N_c and N_f , this evolution and the β function that describes it, depend on three variables: α (and thus, parametrically, μ), N_c , and N_f , while in the LNN limit, they only depend on the two variables $\alpha(\mu)$ and r .

Since the rational numbers \mathbb{Q} are dense in the real numbers \mathbb{R} , it follows that in the LNN limit, one can choose values of N_c and N_f so that the rational number r is arbitrarily close to any non-negative real number. Therefore, henceforth, to arbitrarily good accuracy, we may simply treat r as a real number, and we will do so. As is well-known, in the $N_c \rightarrow \infty$ limit and also in the LNN limit, the gauge group $SU(N_c)$ is effectively equivalent to $U(N_c)$. The use of a large- N limit, where N is the number of components in a spin or field, has been valuable in the past partly because it allowed one to obtain exact results for statistical mechanical models [16] and quantum field theories [13]–[15], [17, 18]. Our purpose in using it here is somewhat different, namely to gain further insight into the above-mentioned approximate universality that is exhibited by calculations of the UV to IR evolution of theories with different N_c and N_f but equal or similar values of r .

As part of our analysis, we will briefly contrast the properties of theories with fermions in the fundamental representation with properties of theories with fermions in higher-dimensional representations. In the case where fermions are in a two-index representation (including the adjoint, and symmetric and antisymmetric rank-2 tensor representations), the condition that is necessary and sufficient to construct a finite $N_c \rightarrow \infty$ limit is to set N_f equal to a (non-negative, integer) constant. This is a result of the fact that the quadratic Casimir invariants T_f and C_f [19] that enter into the coefficients of the beta function grow like (a constant times) N_c as $N_c \rightarrow \infty$. If the fermions are in a representation involving three or more indices, then generically for fixed finite N_f , the fermion contributions dominate over the gauge field contributions to the β function by powers of N_c as $N_c \rightarrow \infty$. For example, for the symmetric rank-3 tensor representation, $T_f \sim N_c^2$ for large N_c , so that the fermion contribution to the leading β function coefficient dominates over the gauge-field contribution, which is $\sim N_c$, spoiling the asymptotic freedom of the theory. Hence, aside from our primary focus on the case of fermions in the funda-

mental representation, we will restrict our discussion of other representations to the adjoint, and symmetric and antisymmetric rank-2 tensors.

By taking r near to its maximum value allowed by asymptotic freedom, one can arrange that the zero of β occurs at an arbitrarily small value of ξ_{IR} , and one may conclude that in the infrared the theory is in a deconfined non-Abelian Coulomb phase without any spontaneous chiral symmetry breaking. In this case, the IR zero of β at ξ_{IR} is an exact fixed point of the renormalization group for the theory. In contrast, as r decreases, ξ_{IR} increases, and studies with finite N_c and N_f lead to the conclusion that for N_f less than a critical value, $N_{f,cr}$, as μ decreases though a value denoted Λ , the interaction strength $\alpha(\mu)$ exceeds a critical value, α_{cr} , to produce spontaneous chiral symmetry breaking and associated dynamical mass generation for the fermions. For a given N_c , the theory may thus be considered to undergo a (zero-temperature) chiral phase transition as N_f passes through this value, $N_{f,cr}$ [20], and there has been an intensive research program using lattice gauge simulations to determine $N_{f,cr}$ for values such as $N_c = 3$ and $N_c = 2$ [21]. Correspondingly, in the LNN limit considered here, the theory undergoes a chiral phase transition as r passes through r_{cr} , where $r_{cr} = N_{f,cr}/N_c$, with the UV to IR evolution leading to a chirally symmetric phase for $r > r_{cr}$ and a phase with spontaneous chiral symmetry breaking for $r < r_{cr}$. If $r < r_{cr}$, then in the effective low-energy field theory below Λ , one integrates out the fermions (which have dynamically generated masses of order Λ), and the β function changes to become that of a pure non-Abelian gauge theory, which does not have a (perturbative) zero. In this case, ξ_{IR} is only an approximate fixed point.

This paper is organized as follows. In Section II we define an appropriately scaled beta function, called β_ξ , that is a finite function of ξ in the LNN limit and in this section, and in Sections III and IV we investigate its structure up to four-loop order. Our results include an analysis of the behavior of the coefficients as functions of r , the LNN limits for the n -loop IR zero, $\xi_{IR,n\ell}$, the value of ξ where β_ξ is a minimum, the value of β_ξ at this minimum, and the derivative $d\beta_\xi/d\xi$ evaluated at $\xi_{IR,n\ell}$. In Section V we carry out a similar analysis of the coefficients in the anomalous dimension of the fermion bilinear, γ_m , and its value at $\xi_{IR,n\ell}$, again up to four-loop order. In Section VI we calculate correction terms to the LNN limits for various quantities and give a general analytic explanation for the rapidity with which this limit is approached, namely that these correction terms are strongly suppressed, by the factor $1/N_c^2$. Section VIII is devoted to a corresponding study of the LNN limit of a supersymmetric gauge theory. Our conclusions are contained in a final section.

II. β FUNCTION AND SOME GENERAL PROPERTIES IN THE LNN LIMIT

A. General

In this section we analyze the β function in the limit (1.2). It will be convenient to define $a(\mu) \equiv g(\mu)^2/(16\pi^2) = \alpha(\mu)/(4\pi)$ and

$$x(\mu) = \frac{\xi(\mu)}{4\pi} . \quad (2.1)$$

(The argument μ will often be suppressed in the notation.) In terms of α , or equivalently, a , the beta function has the series expansion

$$\beta \equiv \beta_\alpha = -8\pi a \sum_{\ell=1}^{\infty} b_\ell a^\ell = -2\alpha \sum_{\ell=1}^{\infty} \bar{b}_\ell \alpha^\ell , \quad (2.2)$$

where ℓ denotes the loop order and $\bar{b}_\ell \equiv b_\ell/(4\pi)^\ell$. Thus, the n -loop beta function is given by Eq. (2.2) with ∞ replaced by n as the upper limit on the summation over loop order, ℓ . The coefficients b_ℓ for $\ell = 1, 2$ are independent of the scheme used for the regularization and renormalization of the theory and were calculated in [3] and [4]. The b_ℓ with $\ell \geq 3$ are scheme-dependent and have been calculated up to $(\ell = 4)$ -loop order [6, 7] in the modified minimal subtraction [22] (\overline{MS}) scheme [23]. The usefulness of the \overline{MS} scheme has been demonstrated, e.g., by the fact that inclusion of three-loop and four-loop corrections in the running of $\alpha_s(\mu)$ in QCD significantly improves the fit to experimental data [24]. The scheme-dependence of the higher-loop IR zero of the beta function was recently studied in [25].

For our present analysis of the theory in the LNN limit, the first step is to construct a beta function that has a finite, nontrivial LNN limit. We do this by multiplying both sides of (2.2) by N_c and then taking the LNN limit. The result is a function of ξ and can be expressed as

$$\beta_\xi \equiv \frac{d\xi}{dt} = \lim_{LNN} \beta_\alpha N_c . \quad (2.3)$$

This function has the expansion

$$\beta_\xi \equiv \frac{d\xi}{dt} = -8\pi x \sum_{\ell=1}^{\infty} \hat{b}_\ell x^\ell = -2\xi \sum_{\ell=1}^{\infty} \tilde{b}_\ell \xi^\ell , \quad (2.4)$$

where

$$\hat{b}_\ell = \lim_{LNN} \frac{b_\ell}{N_c^\ell} , \quad \tilde{b}_\ell = \lim_{LNN} \frac{\bar{b}_\ell}{N_c^\ell} . \quad (2.5)$$

Thus, similarly to the relation between \bar{b}_ℓ and b_ℓ ,

$$\tilde{b}_\ell = \frac{\hat{b}_\ell}{(4\pi)^\ell} . \quad (2.6)$$

As with Eq. (2.5), it is understood here and below that all expressions have been evaluated in the LNN limit (1.2). The β_ξ function, calculated to n -loop ($n\ell$) order, is denoted by $\beta_{\xi,n\ell}$ and is given by Eq. (2.4) with ∞ replaced by n as the upper limit on the sum over ℓ .

To analyze the zeros of $\beta_{\xi,n\ell}$, aside from the double zero at $\xi = x = 0$, we extract an overall factor of $-2\xi^2$ and calculate the zeros of the reduced (r) polynomial

$$\beta_{\xi,n\ell,r} \equiv -\frac{\beta_{\xi,n\ell}}{2\xi^2} = \sum_{\ell=1}^n \tilde{b}_\ell \xi^{\ell-1} = \frac{1}{4\pi} \sum_{\ell=1}^n \hat{b}_\ell x^{\ell-1} . \quad (2.7)$$

As is clear from Eq. (2.7), the zeros of $\beta_{\xi,n\ell}$ away from the origin depend only on $n-1$ ratios of coefficients, which can be taken as \hat{b}_ℓ/\hat{b}_n for $\ell = 1, \dots, n-1$. Although Eq. (2.7) is an algebraic equation of degree $n-1$, with $n-1$ roots, only one of these is physically relevant as the IR zero of $\beta_{\xi,n\ell}$. We denote this as $\xi_{IR,n\ell} = 4\pi x_{IR,n\ell}$.

B. Behavior of Coefficients in β as Functions of r

From the expressions for b_1 and b_2 [3, 4], we have

$$\hat{b}_1 = \frac{1}{3}(11 - 2r) \quad (2.8)$$

and

$$\hat{b}_2 = \frac{1}{3}(34 - 13r) . \quad (2.9)$$

In the \overline{MS} scheme, from the expression for b_3 [6], we obtain

$$\begin{aligned} \hat{b}_3 &= \frac{1}{54}(2857 - 1709r + 112r^2) \\ &= 52.9074 - 31.6481r + 2.07407r^2 \end{aligned} \quad (2.10)$$

and from b_4 [7], we obtain

$$\begin{aligned} \hat{b}_4 &= \frac{150473}{486} - \left(\frac{485513}{1944}\right)r + \left(\frac{8654}{243}\right)r^2 + \left(\frac{130}{243}\right)r^3 + \frac{4}{9}(11 - 5r + 21r^2)\zeta(3) \\ &= 315.492 - 252.421r + 46.832r^2 + 0.534979r^3 , \end{aligned} \quad (2.11)$$

to the indicated numerical floating-point accuracy, where $\zeta(s) = \sum_{n=1}^{\infty} n^{-s}$ is the Riemann ζ function. For some purposes it is more convenient to deal with the \hat{b}_ℓ , since they are free of factors of 4π , while for numerical purposes it is often more convenient to use the \tilde{b}_ℓ , since the range of values of \tilde{b}_ℓ as functions of ℓ is somewhat smaller than the range for the \hat{b}_ℓ . In Table I we list values of \tilde{b}_ℓ for $2 \leq \ell \leq 4$ as functions of r in the interval $0 \leq r \leq r_{b1z}$.

In [9], $N_{f,b\ell z}$ was defined as the value or set of values of N_f where $b_\ell = 0$ and thus, for our present analysis, we define

$$r_{b\ell z} \equiv \lim_{LNN} \frac{N_{f,b\ell z}}{N_c}. \quad (2.12)$$

From Eq. (2.8), we have

$$r_{b1z} = \frac{11}{2}. \quad (2.13)$$

As is evident from Eqs. (2.8) and (2.9), the coefficients \hat{b}_1 and \hat{b}_2 are both monotonically (and linearly) decreasing functions of r . The coefficient \hat{b}_1 decreases from $11/3$ to 0 as r increases from 0 to $r_{b1z} = 11/2$. We require that the theory be asymptotically free, i.e.,

$$r < r_{b1z} = \frac{11}{2}. \quad (2.14)$$

The coefficient \hat{b}_2 decreases from $34/3$ at $r = 0$ and passes through zero to negative values as r increases through the value

$$r_{b2z} = \frac{34}{13}. \quad (2.15)$$

As $r \nearrow r_{b1z}$, \hat{b}_2 reaches the value

$$\hat{b}_2 = -\frac{25}{2} \quad \text{at } r = r_{b1z}. \quad (2.16)$$

Therefore, in the LNN limit, the interval in r , denoted I_r , where the two-loop β_ξ function has an IR zero, is given by

$$I_r : \quad r_{b2z} < r < r_{b1z}, \quad \frac{34}{13} < r < \frac{11}{2} \quad (2.17)$$

(i.e., $2.615 < r < 5.500$). With $r \in I_r$, we will, correspondingly, focus on the UV to IR evolution in the interval

$$I_\xi : \quad 0 \leq \xi(\mu) \leq \xi_{IR,n\ell}. \quad (2.18)$$

The coefficient \hat{b}_3 vanishes at two values of r , denoted

$$r_{b3z1} = \frac{1709 - 57\sqrt{505}}{224} = 1.911 \quad (2.19)$$

and

$$r_{b3z2} = \frac{1709 + 57\sqrt{505}}{224} = 13.348, \quad (2.20)$$

where here and below, the floating-point values are given to the indicated accuracy. This coefficient \hat{b}_3 is monotonically decreasing in the interval $0 < r < r_{b1z}$, decreasing from $\hat{b}_3 = 2857/54 = 52.907$ at $r = 0$ and passing through zero to negative values as r increases through r_{b3z1} in Eq. (2.19). As r increases from r_{b3z1} , \hat{b}_3 continues to decrease and passes through the value

$$\hat{b}_3 = -\frac{5299}{338} = -15.6775 \quad \text{at } r = r_{b2z} = \frac{34}{13} \quad (2.21)$$

at the lower end of the interval I_r . As r increases throughout the interval I_r , \hat{b}_3 decreases further, and as r increases to its maximum, r_{b1z} , at the upper end of this interval, \hat{b}_2 reaches the value

$$\hat{b}_3 = -\frac{701}{12} = -58.417 \quad \text{at } r = r_{b1z} = \frac{11}{2}. \quad (2.22)$$

Since

$$r_{b3z1} < r_{b2z} \quad (2.23)$$

and

$$r_{b3z2} > r_{b1z}, \quad (2.24)$$

it follows that in the \overline{MS} scheme,

$$\hat{b}_3 < 0 \quad \forall \quad r \in I_r. \quad (2.25)$$

Given this result and the fact that the quantity $-54\hat{b}_3$ will appear in later formulas, it will be convenient to denote

$$D_{3\ell} \equiv -54\hat{b}_3 = -2857 + 1709r - 112r^2, \quad (2.26)$$

which is positive for $r \in I_r$.

For completeness, we note that \hat{b}_3 reaches a minimum at $r = 1709/224 = 7.629$, and, for larger r , it increases, passing through zero again at the value r_{b3z2} in Eq. (2.20). Since these values of r lie above r_{b1z} , they are not of direct interest for our present study.

As r increases through the range $0 \leq r < r_{b1z}$, the coefficient \hat{b}_4 in the \overline{MS} scheme decreases from the value

$$\hat{b}_4 = \frac{150473}{486} + \frac{44\zeta(3)}{9} = 315.492 \quad \text{at } r = 0, \quad (2.27)$$

(i.e., $\tilde{b}_4 = 1.265 \times 10^{-2}$), passes through zero with negative slope at

$$r_{b4z,1} = 2.040, \quad (2.28)$$

reaches a minimum of -14.831 at $r = 2.581$, and then increases. At the lower end of the interval I_r , at r_{b2z} ,

$$\hat{b}_4 = -\frac{550009}{6084} + \frac{31900\zeta(3)}{507} = -14.770 \quad \text{at } r = r_{b2z}. \quad (2.29)$$

As r increases in the interval I_r , \hat{b}_4 passes through zero again, at

$$r_{b_{4z},2} = 3.119, \quad (2.30)$$

this time with positive slope, and attains the value

$$\hat{b}_4 = \frac{14731}{144} + 275\zeta(3) = 432.864 \quad \text{at } r = r_{b_{1z}} \quad (2.31)$$

(i.e., $\tilde{b}_4 = 1.736 \times 10^{-2}$) at the upper end of the interval I_r . Some special values, expressed in terms of the \tilde{b}_ℓ coefficients, are listed in Table II.

Concerning the sign of \hat{b}_4 in the range $r \geq 0$,

$$\begin{aligned} \hat{b}_4 &> 0 \quad \text{for } 0 < r < r_{b_{4z},1}, \\ \hat{b}_4 &< 0 \quad \text{for } r_{b_{4z},1} < r < r_{b_{4z},2}, \\ \hat{b}_4 &> 0 \quad \text{for } r_{b_{4z},1} < r < r_{b_{1z}}. \end{aligned} \quad (2.32)$$

That is, numerically, $\hat{b}_4 > 0$ if $0 < r < 2.040$ or $r > 3.119$, and $\hat{b}_4 < 0$ if $2.040 < r < 3.119$. The zero of \hat{b}_4 at $r_{b_{4z},1} = 2.040$ lies below the lower end of the interval I_r (at $r_{b_{2z}} = 2.615$), while the zero at $r_{b_{4z},2} = 3.119$ lies in the interior of the interval I_r . Hence, restricting to $r \in I_r$,

$$\text{For } r \in I_r, \quad \hat{b}_4 < 0 \quad \text{if } r_{b_{2z}} < r < r_{b_{4z},1}$$

$$\hat{b}_4 > 0 \quad \text{if } r_{b_{4z},1} < r < r_{b_{1z}}, \quad (2.33)$$

i.e., numerically, for $r \in I_r$, $\hat{b}_4 < 0$ if $2.615 < r < 3.119$ and $\hat{b}_4 > 0$ if $3.119 < r < 5.500$. Since \hat{b}_4 is a cubic polynomial in r , there is a third value of r where it vanishes, but this is at the negative, and hence unphysical, value $r = -92.699$ and hence is of no direct relevance here. Although our analysis here presumes the LNN limit, a remark is in order for finite N_c and N_f . The interval where \hat{b}_4 is negative for $r \in I_r$ is not present for sufficiently small N_c and N_f . This is evident from the explicit \bar{b}_4 values listed in Table I of our Ref. [9] for $N_c = 2$ and $N_c = 4$. This interval of negative \bar{b}_4 values is present for $N_c \geq 4$.

III. IR ZERO OF β

Combining the results from the previous section, we exhibit the explicit four-loop β_ξ function. For this purpose, it is simplest to use the x variable defined in Eq. (2.1). We have

$$\begin{aligned} \beta_\xi = & -8\pi x^2 \left[\frac{11-2r}{3} + \left(\frac{34-13r}{3} \right) x + \left(\frac{2857-1709r+112r^2}{54} \right) x^2 \right. \\ & \left. + \left\{ \frac{150473}{486} - \left(\frac{485513}{1944} \right) r + \left(\frac{8654}{243} \right) r^2 + \left(\frac{130}{243} \right) r^3 + \frac{4}{9} (11-5r+21r^2) \zeta(3) \right\} x^3 + O(x^4) \right]. \end{aligned} \quad (3.1)$$

A. Two-Loop Level

At the two-loop level, if $r \in I_r$, then β_ξ has an IR zero at

$$\begin{aligned} \xi_{IR,2\ell} &= -\frac{\tilde{b}_1}{\tilde{b}_2} = -\frac{4\pi\hat{b}_1}{\hat{b}_2} \\ &= \frac{4\pi(11-2r)}{13r-34}. \end{aligned} \quad (3.2)$$

Since this is obtained from a perturbative calculation, it is only reliable if $\xi_{IR,2\ell}$ is not too large. As $r \rightarrow r_{b_{1z}}$, $\xi_{IR,2\ell} \rightarrow 0$, and hence in the upper end of the interval I_r , one may plausibly expect that this two-loop expression becomes a progressively more and more accurate approximation to the IR zero of the exact β_ξ function. As $r \searrow 34/13$ at the lower end of the interval I_r , $\xi_{IR,2\ell}$ grows

too large for this perturbative calculation to be applicable. It will be useful here and below to give values of various quantities at an illustrative value of r .

B. Three-Loop Level

At the three-loop level, the IR zero of β_ξ is given by the physical (smallest positive) root of the quadratic equation

$$\beta_{\xi,2\ell,r} = \tilde{b}_1 + \tilde{b}_2 \xi + \tilde{b}_3 \xi^2 = 0. \quad (3.3)$$

This equation has, formally, two solutions, namely

$$\frac{1}{2\tilde{b}_3} \left(-\tilde{b}_2 \pm \sqrt{\tilde{b}_2^2 - 4\tilde{b}_1\tilde{b}_3} \right). \quad (3.4)$$

Since we have shown that $\tilde{b}_3 < 0$ for $r \in I_r$ for a general scheme that preserves the existence of the IR zero in the (scheme-independent) $\beta_{\xi,2\ell}$ at the three-loop level, we can rewrite (3.4) as

$$\frac{1}{2|\tilde{b}_3|} \left(-|\tilde{b}_2| \mp \sqrt{\tilde{b}_2^2 + 4\tilde{b}_1|\tilde{b}_3|} \right). \quad (3.5)$$

As is evident from Eq. (3.5), only the root corresponding to the lower sign choice in Eq. (3.5) is positive and hence physical. We denote it as

$$\xi_{IR,3\ell} = \frac{1}{2|\tilde{b}_3|} \left(-|\tilde{b}_2| + \sqrt{\tilde{b}_2^2 + 4\tilde{b}_1|\tilde{b}_3|} \right). \quad (3.6)$$

By the same type of proof as was given in [9, 12], for the relevant interval $r \in I_r$ where the scheme-independent two-loop $\beta_{\xi,2\ell}$ function has an IR zero, we find that at the three-loop level

$$\xi_{IR,3\ell} \leq \xi_{IR,2\ell} \quad \text{for } r \in I_r, \quad (3.7)$$

with equality only at $r = r_{b1z}$, where $\xi_{IR,3\ell} = \xi_{IR,2\ell} = 0$. In [12] we pointed out that the corresponding inequality $\alpha_{IR,3\ell} < \alpha_{IR,2\ell}$ applies more generally than just in the \overline{MS} scheme, and the same is true of the inequality (3.7). We recall the reasoning for this. Since the existence of an IR zero in the two-loop β function, $\beta_{\xi,2\ell}$, is a scheme-independent property of the theory, a reasonable scheme should maintain the existence of this IR zero (albeit with a shifted value) at higher-loop order. Now in order for a scheme to maintain this zero, a necessary and sufficient condition is that $\tilde{b}_2^2 - 4\tilde{b}_1\tilde{b}_3 \geq 0$, so that the square root in Eq. (3.4) is real. But the lower end of the interval I_r is defined by the condition that $\tilde{b}_2 \rightarrow 0$ as $r \searrow r_{b2z}$. Given that $r \in I_r$ so $\beta_{\xi,2\ell}$ has an IR zero, this means that a reasonable scheme, which preserves the existence of this zero at the three-loop level, should have $\tilde{b}_3 < 0$ for $r \in I_r$. From this, by the same type of proof as was given in [12] for this class of schemes, the inequality (3.7) follows.

Substituting the relevant expressions for the \tilde{b}_ℓ in (3.6), we have, in the \overline{MS} scheme, the explicit result

$$\xi_{IR,3\ell} = \frac{12\pi[-3(13r-34) + \sqrt{C_{3\ell}}]}{D_{3\ell}}, \quad (3.8)$$

where $D_{3\ell}$ was defined above in Eq. (2.26), and it is convenient to define the shorthand notation

$$C_{3\ell} = -52450 + 41070r - 7779r^2 + 448r^3. \quad (3.9)$$

The polynomial $C_{3\ell}$ has only one real zero, at $r = 1.86532$ (to the indicated accuracy) and is positive for $r > 1.86532$, and hence for all $r \in I_r$. The polynomial $-3(13r-34)$ vanishes at the lower end of the interval I_r and is negative for $r \in I_r$, but it is smaller than $\sqrt{C_{3\ell}}$, so $\xi_{IR,3\ell} > 0$ for $r \in I_r$, as is necessary for it to be physical.

In Table III we list numerical values of $\xi_{IR,2\ell}$ and $\xi_{IR,3\ell}$ for $r \in I_r$. As is evident in this table, $\xi_{IR,2\ell}$ and $\xi_{IR,3\ell}$

decrease monotonically as a function of r throughout this interval I_r (as does $\xi_{IR,4\ell}$, to be discussed below). At the lower end of this interval,

$$\xi_{IR,3\ell} = 20\pi\sqrt{\frac{26}{5299}} = 4.401 \quad \text{at } r = \frac{34}{13}, \quad (3.10)$$

and at the upper end,

$$\xi_{IR,3\ell} \rightarrow 0 \quad \text{as } r \nearrow r_{b1z} = \frac{11}{2}. \quad (3.11)$$

The ratio $\xi_{IR,3\ell}/\xi_{IR,2\ell}$ increases monotonically from 0 as r increases from the value $r = 34/13$ at the lower end of the interval I_r , and this ratio approaches 1 from below as r approaches the upper end of the interval I_r at $r = 11/2$. It is useful here and below to give illustrative values of various quantities and ratios at an illustrative value of r . For this purpose, we choose an r approximately in the middle of the I_r , namely $r = 4$. We have

$$\xi_{IR,2\ell}|_{r=4} = \frac{2\pi}{3} = 2.0944 \quad (3.12)$$

and

$$\xi_{IR,3\ell}|_{r=4} = \frac{4\pi(-2 + \sqrt{22})}{27} = 1.2522 \quad (3.13)$$

so that

$$\frac{\xi_{IR,3\ell}}{\xi_{IR,2\ell}} \Big|_{r=4} = \frac{2(-2 + \sqrt{22})}{9} = 0.5979. \quad (3.14)$$

This ratio provides an illustrative measure of the decrease in the value of the IR zero of β when one calculates it at three-loop order, as compared with two-loop order.

C. Four-Loop Level

At the four-loop level, the IR zero of β_ξ is the (smallest positive) root of the cubic equation

$$\beta_{\xi,4\ell,r} \equiv \tilde{b}_1 + \tilde{b}_2\xi + \tilde{b}_3\xi^2 + \tilde{b}_4\xi^3 = 0. \quad (3.15)$$

Now $\tilde{b}_2 < 0$ for $r \in I_r$, and we recall our discussion above, that $\tilde{b}_3 < 0$ for $r \in I_r$ in the \overline{MS} scheme and other schemes that maintain the existence of the IR zero in $\beta_{\xi,2\ell}$ at the three-loop level. We can therefore write Eq. (3.15) as

$$\tilde{b}_1 - |\tilde{b}_2|\xi - |\tilde{b}_3|\xi^2 + \tilde{b}_4\xi^3 = 0. \quad (3.16)$$

For $r \in I_r$, Eq. (3.15), or equivalently, (3.16), has three real roots, and from these we determine the relevant (smallest, positive) one as $\xi_{IR,4\ell}$. We list values of $\xi_{IR,4\ell}$ in Table III.

D. Shift of IR Zero From n -Loop to $(n+1)$ -Loop Level

In [12], a general result was derived concerning the sign of the shift of the IR zero of β going from the n -loop level to the $(n+1)$ -loop level. Provided the scheme has the property that b_ℓ with $\ell \geq 3$ are such as to maintain the existence of the zero in the two-loop β function, then $\alpha_{IR,(n+1)\ell} > \alpha_{IR,n\ell}$ if $b_{n+1} > 0$ and $\alpha_{IR,(n+1)\ell} < \alpha_{IR,n\ell}$ if $b_{n+1} < 0$. The same proof can be applied here to deduce that, provided that the scheme has the property that \hat{b}_ℓ with $\ell \geq 3$ are such as to maintain the existence of the zero in the two-loop β_ξ function, then

$$\begin{aligned} \xi_{IR,(n+1)\ell} &> \xi_{IR,n\ell} \quad \text{if } \hat{b}_{n+1} > 0, \\ \xi_{IR,(n+1)\ell} &< \alpha_{IR,n\ell} \quad \text{if } \hat{b}_{n+1} < 0. \end{aligned} \quad (3.17)$$

We may apply this inequality for the comparisons of $\xi_{IR,3\ell}$ with $\xi_{IR,2\ell}$ and $\xi_{IR,4\ell}$ with $\xi_{IR,3\ell}$. Since $\hat{b}_3 < 0$ for $r \in I_r$, this result provides another way of deducing the inequality (3.7) for the two-loop versus three-loop comparison. Applying the general inequality for the three-loop versus four-loop comparison, we infer that

$$\begin{aligned} \xi_{IR,4\ell} &< \xi_{IR,3\ell} \quad \text{if } 2.615 < r < 3.119, \text{ so } \tilde{b}_4 < 0, \\ \xi_{IR,4\ell} &> \xi_{IR,3\ell} \quad \text{if } 3.119 < r < 5.500, \text{ so } \tilde{b}_4 > 0. \end{aligned} \quad (3.18)$$

These inequalities are evident in Table III. For example, at $r = 3.0$, $\xi_{IR,4\ell}/\xi_{IR,3\ell} = 0.976$, while for $r = 5.0$, $\xi_{IR,4\ell}/\xi_{IR,3\ell} = 1.02$. One sees that the magnitude of the fractional difference

$$\frac{|\xi_{IR,4\ell} - \xi_{IR,3\ell}|}{\xi_{IR,4\ell}} \quad (3.19)$$

is reasonably small. This is in agreement with one's general expectation that if a perturbative calculation is reliable, then as one calculates this quantity to progressively higher-loop order, the magnitudes of the fractional differences between the values at the n 'th and $(n+1)$ 'th orders should decrease.

E. Summary of Results on IR Zero of β_ξ

We summarize our findings concerning $\xi_{IR,n\ell}$ as follows. As one goes from the (scheme-independent) two-loop level to the three-loop level, the value of the IR zero of β_ξ decreases. For r in the lower part of the interval I_r where the two-loop β_ξ function has an IR zero, this reduction in the value of the IR zero is rather substantial. For example, for $r = 3.0$, near the lower end of the

interval I_r , $\xi_{IR,3\ell}/\xi_{IR,2\ell} = 0.234$, while for $r = 5.0$, near the upper end of I_r , $\xi_{IR,3\ell}/\xi_{IR,2\ell} = 0.873$. Going from three-loop to four-loop order, the change in the value of the IR zero is smaller in magnitude and can be of either sign, depending on the value of $r \in I_r$. In general, both $\xi_{IR,3\ell}$ and $\xi_{IR,4\ell}$ are smaller than $\xi_{IR,2\ell}$.

IV. SOME STRUCTURAL PROPERTIES OF β_ξ

For theories which exhibit an IR zero, $\xi_{IR,2\ell}$, in the two-loop beta function, $\beta_{\xi,2\ell}$, there are several structural properties of interest in addition to higher-loop values of this IR zero. These include

- the value of ξ at which $\beta_{\xi,n\ell}$ reaches a minimum in the interval I_ξ , denoted $\xi_{m,n\ell}$, where the subscript m denotes minimum
- the value of $\beta_{\xi,n\ell}$ at this minimum, denoted $(\beta_{\xi,n\ell})_{min}$
- the derivative of $\beta_{\xi,n\ell}$ at $\xi_{IR,n\ell}$, denoted

$$\beta'_{\xi,IR,n\ell} \equiv \left. \frac{d\beta_{\xi,n\ell}}{d\xi} \right|_{\xi=\xi_{IR,n\ell}}. \quad (4.1)$$

Note that because $\xi = \alpha N_c$ and $\beta_\xi = \lim_{LNN} \beta_\alpha N_c$, the factor of N_c divides out in the derivative $d\beta_\xi/d\xi$, so that

$$\frac{d\beta_\xi}{d\xi} = \lim_{LNN} \frac{d\beta_\alpha}{d\alpha}, \quad (4.2)$$

and

$$\frac{d\beta_{\xi,n\ell}}{d\xi} = \lim_{LNN} \frac{d\beta_{\alpha,n\ell}}{d\alpha}, \quad (4.3)$$

In particular,

$$\left. \frac{d\beta_{\xi,n\ell}}{d\xi} \right|_{\xi=\xi_{IR,n\ell}} = \lim_{LNN} \left. \frac{d\beta_{\alpha,n\ell}}{d\alpha} \right|_{\alpha=\alpha_{IR,n\ell}}. \quad (4.4)$$

As was discussed in [12], higher-loop calculations of the derivative $\left. \frac{d\beta_{\alpha,n\ell}}{d\alpha} \right|_{\alpha=\alpha_{IR,n\ell}}$ are of interest because this enters into estimates of a dilaton mass in a quasiconformal gauge theory. In turn, this also provides one motivation for studying the LNN limit of this derivative, $\left. \frac{d\beta_{\xi,n\ell}}{d\xi} \right|_{\xi=\xi_{IR,n\ell}}$.

A. Position of Minimum in $\beta_{\xi,n\ell}$

Concerning the position of the minimum in β_ξ for $r \in I_r$, we calculate that at the two-loop level,

$$\xi_{m,2\ell} = \frac{8\pi(11-2r)}{3(13r-34)}. \quad (4.5)$$

This satisfies

$$\xi_{m,2\ell} = \frac{2}{3}\xi_{IR,2\ell}. \quad (4.6)$$

At the three-loop level in the \overline{MS} scheme, we find

$$\xi_{m,3\ell} = \frac{3\pi[-9(13r-34) + \sqrt{E_{3\ell}}]}{D_{3\ell}}, \quad (4.7)$$

where we define the shorthand notation

$$E_{3\ell} = -409196 + 320604r - 60711r^2 + 3584r^3. \quad (4.8)$$

From Eqs. (3.8) and (4.7), we find

$$\frac{\xi_{m,3\ell}}{\xi_{IR,3\ell}} = \frac{-9(13r-34) + \sqrt{E_{3\ell}}}{4[-3(13r-34) + \sqrt{C_{3\ell}}]}. \quad (4.9)$$

This may be compared with the corresponding ratio of two-loop quantities $\xi_{m,2\ell}/\xi_{IR,2\ell} = 2/3$. In contrast to the latter ratio, which is a constant, independent of $r \in I_r$, the ratio (4.9) is a monotonically decreasing function of $r \in I_r$. At the lower end of this interval,

$$\frac{\xi_{m,3\ell}}{\xi_{IR,3\ell}} = \frac{1}{\sqrt{2}} \quad \text{at } r = r_{b2z} = \frac{34}{13}. \quad (4.10)$$

As r approaches the upper end of the I_r at $r_{b1z} = 11/2$, the ratio (4.9) approaches the limit

$$\lim_{r \nearrow r_{b1z}} \frac{\xi_{m,3\ell}}{\xi_{IR,3\ell}} = \frac{2}{3}. \quad (4.11)$$

Note that both $\xi_{m,3\ell}$ and $\xi_{IR,3\ell}$ individually approach zero as $r \nearrow 11/2$, although their ratio in Eq. (4.11) approaches a constant.

Illustrative values in the LNN limit for $r = 4$ are

$$\xi_{m,2\ell}|_{r=4} = \frac{4\pi}{9} = 1.396. \quad (4.12)$$

and

$$\xi_{m,3\ell}|_{r=4} = \frac{2\pi(-1 + \sqrt{5})}{9} = 0.8629. \quad (4.13)$$

so that for this value, $r = 4$, in addition to the ratio $\xi_{m,2\ell}/\xi_{IR,2\ell} = 2/3$, we have

$$\frac{\xi_{m,3\ell}}{\xi_{IR,3\ell}} \Big|_{r=4} = \frac{3}{2} \left(\frac{-1 + \sqrt{5}}{-2 + \sqrt{22}} \right) = 0.68915. \quad (4.14)$$

and

$$\frac{\xi_{m,3\ell}}{\xi_{m,2\ell}} = \frac{-1 + \sqrt{5}}{2} = 0.6180. \quad (4.15)$$

B. Value of $\beta_{\xi,n\ell}$ at Minimum

We calculate the following minimum values of $\beta_{\xi,n\ell}$ as a function of $r \in I_r$:

$$(\beta_{\xi,2\ell})_{min} = -\frac{2^5\pi(11-2r)^3}{3^4(13r-34)^2} \quad (4.16)$$

and

$$(\beta_{\xi,3\ell})_{min} = -\frac{3\pi(F_{3\ell} + G_{3\ell}\sqrt{E_{3\ell}})}{8D_{3\ell}^3}, \quad (4.17)$$

where $D_{3\ell}$ and $E_{3\ell}$ were defined above in Eqs. (2.26) and (4.8). The functions $F_{3\ell}$ and $G_{3\ell}$ are given in the appendix.

For the illustrative value $r = 4$,

$$(\beta_{\xi,2\ell})_{min} = -\frac{2^3\pi}{3^5} = -0.1034 \quad (4.18)$$

and

$$(\beta_{\xi,3\ell})_{min} = -\frac{2\pi(13-5\sqrt{5})}{3^5} = -0.04705. \quad (4.19)$$

C. $d\beta_{\xi,n\ell}/d\xi$ at $\xi_{IR,n\ell}$

At the two-loop level, we calculate

$$\beta'_{\xi,IR,2\ell} = \frac{2(11-2r)^2}{3(13r-34)}. \quad (4.20)$$

This is clearly positive for $r \in I_r$, approaching zero as r approaches the upper end of this interval at $r = r_{b1z}$. At the three-loop level, we find

$$\beta'_{\xi,IR,3\ell} = \frac{4[-3(13r-34)C_{3\ell} + K_{3\ell}\sqrt{C_{3\ell}}]}{D_{3\ell}^2}, \quad (4.21)$$

where $C_{3\ell}$ and $D_{3\ell}$ were defined above in Eqs. (3.9) and (2.26), and we define

$$K_{3\ell} = -21023 + 16557r - 3129r^2 + 224r^3. \quad (4.22)$$

The first term in the numerator, $-3(13r-34)C_{3\ell}$, is negative for $r \in I_r$, but is smaller in magnitude than the second term, $K_{3\ell}\sqrt{C_{3\ell}}$. This shows analytically that $\beta'_{\xi,IR,3\ell} > 0$ for $r \in I_r$. The positivity of $\beta'_{\xi,IR,n\ell}$ for $r \in I_r$ is obvious from the graph of $\beta_{\xi,n\ell}$. Since this function is continuous, is negative for $0 < \xi < \xi_{IR,n\ell}$, and has, generically, a simple zero at $\beta'_{\xi,n\ell} > 0$, it follows that $\beta'_{\xi,n\ell} > 0$ for $r \in I_r$. We have also calculated $\beta'_{\xi,IR,4\ell}$ analytically, but the expression is somewhat cumbersome, since it involves cube roots, so we do not list it. Illustrative results of these ratios for the LNN limit and the typical value, $r = 4$, are

$$\beta'_{\xi,IR,2\ell}|_{r=4} = \frac{1}{3}, \quad (4.23)$$

and

$$\beta'_{\xi,IR,3\ell}|_{r=4} = \frac{4(-44 + 13\sqrt{22})}{3^5} = 0.2794. \quad (4.24)$$

This illustrates how the slope of the β_{ξ} function at the n -loop IR zero decreases as it is calculated to three-loop order, as compared with the 2-loop calculation. This is also shown by the explicit numerical results in the tables going up to four-loop order.

V. ANOMALOUS DIMENSION γ_m

The anomalous dimension γ_m describes the scaling of a fermion bilinear and the running of a dynamically generated fermion mass in the phase with spontaneous chiral symmetry breaking. γ_m is defined as $\gamma_m = d \ln Z_m / dt$, where Z_m is the corresponding renormalization constant for the fermion bilinear operator. In the non-Abelian Coulomb phase (which is a conformal phase), the IR zero of β is exact, although a calculation of it to a finite-order in perturbation theory is only approximate, and γ_m evaluated at this IR fixed point is exact. In the phase with spontaneous chiral symmetry breaking, where an IR fixed point, if it exists, is only approximate, γ_m is an effective quantity describing the running of a dynamically generated fermion mass for the evolution of the theory near this approximate IRFP. As in [9, 12], for notational simplicity we will often suppress the subscript m on γ_m where the meaning is clear.

This anomalous dimension can be expressed as a series in a or equivalently, ξ :

$$\gamma \equiv \gamma_m = \sum_{\ell=1}^{\infty} c_{\ell} a^{\ell} = \sum_{\ell=1}^{\infty} \bar{c}_{\ell} \alpha^{\ell}, \quad (5.1)$$

where ℓ denotes the loop order and $\bar{c}_{\ell} = c_{\ell}/(4\pi)^{\ell}$ is the ℓ -loop series coefficient. The coefficient c_1 is scheme-independent while the c_{ℓ} with $\ell \geq 2$ are scheme-dependent. The c_{ℓ} have been calculated up to $\ell = 4$ in the \overline{MS} scheme [26]. The n -loop expression for γ is denoted $\gamma_{n\ell}$ and is given by Eq. (5.1) with ∞ replaced by n as the upper limit on the summation over ℓ . In [9] we evaluated γ to three- and four-loop order at the IR zero of β calculated to the same order and showed that these higher-loop results were somewhat smaller than the two-loop evaluation. In [25] we discussed scheme transformations at an IR fixed point and implications, including those for the scheme-dependence of γ .

In the IR-conformal phase, unitarity implies a lower limit on the dimension of a spinless operator \mathcal{O} , namely, $D_{\mathcal{O}} \geq (d-2)/2$, where d is the spacetime dimension [27]. With our sign convention,

$$D_{\bar{\psi}\psi} = 3 - \gamma, \quad (5.2)$$

so that in this IR-conformal phase, γ is bounded above as

$$\gamma \leq 2. \quad (5.3) \quad \text{and}$$

In the IR phase with confinement and spontaneous chiral symmetry breaking, the dynamical mass generated for the fermions behaves, for Euclidean momentum large compared with the chiral-symmetry-breaking scale, Λ , as $\Sigma(k) \propto \Lambda(\Lambda/k)^{2-\gamma}$ (up to a logarithmic factor) for $k \gg \Lambda$. Hence, the upper bound (5.3) also applies in this phase.

For our present analysis of the LNN limit, we reexpress γ in terms of x or equivalently, ξ :

$$\gamma = \sum_{\ell=1}^{\infty} \hat{c}_{\ell} x^{\ell} = \sum_{\ell=1}^{\infty} \tilde{c}_{\ell} \xi^{\ell}, \quad (5.4)$$

where

$$\hat{c}_{\ell} = \lim_{LNN} \frac{c_{\ell}}{N_c^{\ell}} \quad (5.5)$$

and

$$\tilde{c}_{\ell} = \lim_{LNN} \frac{\bar{c}_{\ell}}{N_c^{\ell}}. \quad (5.6)$$

Thus, similarly to the relation between \bar{c}_{ℓ} and c_{ℓ} ,

$$\tilde{c}_{\ell} = \frac{\hat{c}_{\ell}}{(4\pi)^{\ell}}. \quad (5.7)$$

The n -loop expression for γ is given by the right-hand side of Eq. (5.4) with the sum running from $\ell = 1$ to $\ell = n$ rather than $\ell = \infty$.

In the LNN limit we find

$$\hat{c}_1 = 3 \quad (5.8)$$

$$\hat{c}_2 = \frac{203}{12} - \frac{5}{3}r \quad (5.9)$$

$$\begin{aligned} \hat{c}_3 &= \frac{11413}{108} - \left(\frac{1177}{54} + 12\zeta(3) \right) r - \frac{35}{27}r^2 \\ &= 105.676 - 36.221r - 1.296r^2 \end{aligned} \quad (5.10)$$

and

$$\begin{aligned} \hat{c}_4 &= \frac{460151}{576} - \frac{23816}{81}r + \frac{899}{162}r^2 - \frac{83}{81}r^3 + \left(\frac{1157}{9} - \frac{889}{3}r + 20r^2 + \frac{16}{9}r^3 \right) \zeta(3) \\ &\quad + r(66 - 12r)\zeta(4) + (-220 + 160r)\zeta(5) \\ &= 725.280 - 412.892r + 16.603r^2 + 1.1123r^3, \end{aligned} \quad (5.11)$$

where the floating-point numerical results are given to the indicated accuracy. We list numerical values of the corresponding coefficients \tilde{c}_ℓ for $1 \leq \ell \leq 4$ in Table IV.

In [9], the value of $\gamma_{n\ell}$ evaluated at $\alpha = \alpha_{IR,n\ell}$ was denoted as $\gamma_{IR,n\ell}$ and, analogously, here, in the LNN limit, we define

$$\gamma_{IR,n\ell} \equiv \gamma_{n\ell} \Big|_{\xi=\xi_{IR,n\ell}}. \quad (5.12)$$

At the two-loop level, in terms of the coefficients of β and γ_m , taking into account that $\hat{b}_2 < 0$ for $r \in I_r$,

$$\gamma_{IR,2\ell} = \frac{\hat{b}_1(\hat{c}_1|\hat{b}_2| + \hat{c}_2\hat{b}_1)}{\hat{b}_2^2}. \quad (5.13)$$

Note that the sum of the ℓ -values of the products of coefficients in the denominator of the expression for $\gamma_{IR,2\ell}$ is equal to the sum of the ℓ -values of the coefficients in the numerator. In this case, this sum is 4. Because of this homogeneity property and the relations in Eqs. (2.6) and (5.7), it follows that $\gamma_{IR,2\ell}$ has the same form as Eq. (5.13) if one replaces each \hat{b}_ℓ by \tilde{b}_ℓ and each \hat{c}_ℓ by \tilde{c}_ℓ . Explicitly [9],

$$\gamma_{IR,2\ell} = \frac{(11-2r)(1009-158r+40r^2)}{12(13r-34)^2}. \quad (5.14)$$

$$\gamma_{IR,3\ell} = \frac{1}{4|\hat{b}_3|^3} \left[-|\hat{b}_2| + \sqrt{\hat{b}_2^2 + 4\hat{b}_1|\hat{b}_3|} \right] \left[2\hat{c}_1|\hat{b}_3|^2 + \hat{c}_2|\hat{b}_2||\hat{b}_3| - \hat{c}_3(\hat{b}_2^2 + 2\hat{b}_1|\hat{b}_3|) + (-\hat{c}_2|\hat{b}_3| + \hat{c}_3|\hat{b}_2|)\sqrt{\hat{b}_2^2 + 4\hat{b}_1|\hat{b}_3|} \right]. \quad (5.16)$$

Thus, $\gamma_{IR,3\ell}$ has the same type of homogeneity property as a function of the \hat{b}_ℓ and \hat{c}_ℓ coefficients as we discussed for $\gamma_{IR,2\ell}$. Hence, $\gamma_{IR,3\ell}$ is identically expressed by replacing each \hat{b}_ℓ by \tilde{b}_ℓ and each \hat{c}_ℓ by \tilde{c}_ℓ in Eq. (5.16). Inserting the explicit expressions for the \hat{b}_ℓ and \hat{c}_ℓ then yields the explicit result as a function of r . For the present work we have also calculated the four-loop anomalous dimensions evaluated at the IR zero of β_ξ evaluated to the same order, $\gamma_{IR,4\ell}$.

We list numerical values of these quantities in Table V. We find that, as was the case with $\gamma_{IR,2\ell}$, $\gamma_{IR,3\ell}$ decreases monotonically as r increases from r_{b2z} at the lower end of the interval I_r to zero at $r = r_{b1z}$ at the upper end of this interval. At $r = r_{b2z}$, $\gamma_{IR,3\ell} = 2.680$, and hence the value of $\xi_{IR,3\ell}$ is evidently too large for the (perturbative) calculation of this anomalous dimension to be reliable. $\gamma_{IR,3\ell}$ decreases through the value 2 as r increases through the value 2.73, and $\gamma_{IR,3\ell}$ decreases further through the value 1 as r increases through 3.09. Just as was true of particular values of N_c and N_f [9],

This $\gamma_{IR,2\ell}$ decreases monotonically as r increases from $r_{b2z} = 34/13$ at the lower end of the interval I_r to zero at $r = r_{b1z} = 11/2$ at the upper end of this interval. Because of the upper bound (5.3), if the value of γ calculated via this truncated perturbative expansion is greater than 2, then it is unphysical. This applies, in particular, to the divergence in $\gamma_{IR,2\ell}$ at $r = r_{b2z}$. We find that in the relevant interval I_r , $\gamma_{IR,2\ell}$ exceeds 2 as r decreases below the value 3.569. Thus, we cannot use the formula (5.14) for $r < 3.569$, and it is subject to large corrections unless r is substantially above this value. For reference, we find that $\gamma_{IR,2\ell}$ exceeds 1 as r decreases below the value $r = 3.879$.

At the three-loop level,

$$\gamma_{IR,3\ell} = x(\hat{c}_1 + \hat{c}_2x + \hat{c}_3x^2) \Big|_{x=x_{IR,3\ell}}. \quad (5.15)$$

Substituting $x_{IR,3\ell} = \xi_{IR,3\ell}/(4\pi)$ from Eq. (3.6) and using the property that $\hat{b}_2 < 0$ for $r \in I_r$ and, as discussed above, the property that $\hat{b}_3 < 0$ in a scheme that preserves the existence of the IR zero in the (scheme-independent) $\beta_{\xi,2\ell}$ at the three-loop level, we can write $\gamma_{IR,3\ell}$ in terms of positive quantities as

here, for a given value of r ,

$$\gamma_{IR,3\ell} \leq \gamma_{IR,2\ell}, \quad (5.17)$$

with equality only at $r = r_{b1z}$, where $\gamma_{IR,3\ell} = \gamma_{IR,2\ell} = 0$.

VI. APPROACH TO THE LNN LIMIT

One of the motivations for the present work on calculations of the IR zero, the various structural properties of β , and the anomalous dimension γ evaluated at the IR zero in the LNN limit is that the results provide an understanding of (i) the approximate universality that is exhibited by calculations of these quantities for theories with different values of N_c and N_f such that the respective values of r are the same or nearly the same, and (ii) the fact that this approximate universality occurs even for moderate values of N_c and N_f . As we have shown above, the quantities

- $\alpha_{IR,n\ell}N_c$
- $\alpha_{m,n\ell}N_c$

- $(\beta_{\alpha,n\ell})_{\min} N_c$
- $\left. \frac{d\beta_{IR,n\ell}}{d\alpha} \right|_{\alpha=\alpha_{IR,n\ell}}$
- $\left. \gamma_{n\ell} \right|_{\alpha=\alpha_{IR,n\ell}}$

are finite in the LNN limit, and we will next show that they approach their respective LNN limiting values, namely

- $\xi_{IR,n\ell}$
- $\xi_{m,n\ell}$
- $(\beta_{\xi,n\ell})_{\min}$
- $\left. \frac{d\beta_{\xi,n\ell}}{d\xi} \right|_{\xi=\xi_{IR,n\ell}}$
- $\left. \gamma_{n\ell} \right|_{\xi=\xi_{IR,n\ell}}$

rather rapidly as N_c increases (with $r = N_f/N_c$ fixed). The reason for this is that the largest correction terms to the respective LNN limits for these quantities are of order $1/N_c^2$ and hence are rather strongly suppressed even for moderate values of N_c and N_f . In turn, this is a consequence of the N_c -dependence of the relevant group invariants for fermions in the fundamental representation,

in particular, the Casimir invariant $C_f = (N_c^2 - 1)/(2N_c)$ [19].

We first exhibit the structure of the correction terms for the coefficients in the beta function and anomalous dimension γ . Multiplying by the appropriate inverse powers of N_c to obtain finite results in the LNN limit, we thus consider b_ℓ/N_c^ℓ and c_ℓ/N_c^ℓ . These are polynomials in r and in the variable $1/N_c^2$. We find the following explicit results for correction terms:

$$\frac{b_1}{N_c} = \hat{b}_1 \quad (6.1)$$

$$\frac{b_2}{N_c^2} = \hat{b}_2 + \frac{r}{N_c^2} \quad (6.2)$$

$$\frac{b_3}{N_c^3} = \hat{b}_3 + \frac{11r(17-2r)}{36N_c^2} + \frac{r}{4N_c^4} \quad (6.3)$$

and

$$\begin{aligned} \frac{b_4}{N_c^4} = & \hat{b}_4 + \frac{1}{N_c^2} \left[-\frac{40}{3} + \frac{58583r}{1944} - \frac{2477r^2}{243} - \frac{77r^3}{243} + \left(352 - \frac{548r}{9} - \frac{64r^2}{9} \right) \zeta(3) \right] \\ & + \frac{r}{N_c^4} \left[-\frac{2341}{216} - \frac{623r}{54} + \frac{4}{9}(11+61r)\zeta(3) \right] - \frac{23r}{8N_c^6}. \end{aligned} \quad (6.4)$$

For the ratios c_ℓ/N_c^ℓ we find

$$\frac{c_1}{N_c} = \hat{c}_1 - \frac{3}{N_c^2} \quad (6.5)$$

$$\frac{c_2}{N_c^2} = \hat{c}_2 + \frac{-53+5r}{3N_c^2} + \frac{3}{4N_c^4} \quad (6.6)$$

and

$$\begin{aligned} \frac{c_3}{N_c^3} = & \hat{c}_3 + \frac{1}{N_c^2} \left(-\frac{26309}{216} + \frac{899}{27}r + \frac{35}{27}r^2 \right) \\ & + \frac{1}{N_c^4} \left(\frac{129}{4} - \frac{23r}{2} + 12\zeta(3)r \right) - \frac{129}{8N_c^6}. \end{aligned} \quad (6.7)$$

The corresponding result for c_4 is given in the appendix. As noted, these expansions exhibit the feature that the largest subleading term is smaller than the leading term by a factor of $1/N_c^2$ in the LNN limit.

Similarly, the approach of the product $\alpha_{IR,2\ell}N_c$ to its LNN limit, $\xi_{IR,2\ell}$, has the form

$$\alpha_{IR,2\ell}N_c = \frac{4\pi(11-2r)}{13r-34} + \frac{12\pi r(11-2r)}{(34-13r)^2 N_c^2} + O\left(\frac{1}{N_c^4}\right), \quad (6.8)$$

where the first term on the right-hand side is the LNN limit, $\xi_{IR,2\ell}$, given in Eq. (3.2). Similarly, the two-loop anomalous dimension γ_m , evaluated at the IR zero of the two-loop β function, has the expansion

$$\begin{aligned} \gamma_{IR,2\ell} = & \frac{(11-2r)(1009-158r+40r^2)}{12(13r-34)^2} \\ & + \frac{(11-2r)(18836-5331r+648r^2-140r^3)}{(13r-34)^3 N_c^2} + O\left(\frac{1}{N_c^4}\right). \end{aligned} \quad (6.9)$$

where the first term on the right-hand side is the LNN limit, given in Eq. (5.14). Similar results hold for the

expressions calculated to higher-loop orders. Analogous results concerning correction terms to LNN limits apply to the theory with $\mathcal{N} = 1$ supersymmetry, as will be clear from our discussion below.

We next give some numerical results illustrating the rapidity of approach to the LNN limit. For definiteness, we consider two cases: $N_c = 3$, $N_f = 12$, so $r = 4$, and $N_c = 3$, $N_f = 15$, so $r = 5$. For the first case, $N_c = 3$, $N_f = 12$, the two-loop, three-loop, and four-loop values of the IR zero of β are

$$\alpha_{IR,2\ell} = 0.7540, \quad \alpha_{IR,3\ell} = 0.4349, \quad \alpha_{IR,4\ell} = 0.4704. \quad (6.10)$$

(In Table III of [9] these were listed to three significant figures; here we list them to higher accuracy to compare with the estimates from the LNN limit.) To compute the LNN approximations to $\alpha_{IR,n\ell}$ calculated for a specific N_c and $N_f = rN_c$, we take the corresponding values for $\xi_{IR,n\ell}$ from Table III and divide by N_c , obtaining the result

$$\alpha_{IR,n\ell,L} \equiv \frac{\xi_{IR,n\ell}}{N_c} \quad \text{for fixed } r, \quad (6.11)$$

where the subscript L indicates the LNN origin of the estimate. These approximations become progressively more accurate as N_c gets large for fixed r , but as we will show, they are already quite close to the actual values in Eq. (6.10). We obtain

$$\alpha_{IR,2\ell,L} = 0.6982, \quad \alpha_{IR,3\ell,L} = 0.4713, \quad \alpha_{IR,4\ell,L} = 0.4497 \quad (6.12)$$

Hence, for this $N_c = 3$, $N_f = 12$ case, we find

$$\frac{\alpha_{IR,2\ell}}{\alpha_{IR,2\ell,L}} = 1.080, \quad \frac{\alpha_{IR,3\ell}}{\alpha_{IR,3\ell,L}} = 1.042, \quad \frac{\alpha_{IR,4\ell}}{\alpha_{IR,4\ell,L}} = 1.046, \quad (6.13)$$

Carrying out the corresponding analysis for $N_c = 3$, $N_f = 15$, we calculate

$$\frac{\alpha_{IR,2\ell}}{\alpha_{IR,2\ell,L}} = 1.057, \quad \frac{\alpha_{IR,3\ell}}{\alpha_{IR,3\ell,L}} = 1.046, \quad \frac{\alpha_{IR,4\ell}}{\alpha_{IR,4\ell,L}} = 1.046. \quad (6.14)$$

We next perform the corresponding numerical comparisons for $\gamma_{IR,n\ell}$ at the two-loop, three-loop, and four-loop levels. For $N_c = 3$ and $N_f = 12$,

$$\gamma_{IR,2\ell} = 0.7728, \quad \gamma_{IR,3\ell} = 0.31175, \quad \gamma_{IR,4\ell} = 0.2533. \quad (6.15)$$

(In Table VI of [9] these were listed to three significant figures; here we list them to higher accuracy to compare with the estimates from the LNN limit.) The LNN values of $\gamma_{IR,n\ell}$ are displayed in Table V. Comparing these with the values in Eq. (6.15), we find, for this $N_c = 3$, $N_f = 12$ case, the ratios

$$\frac{\gamma_{IR,2\ell}}{\gamma_{IR,2\ell,L}} = 0.985, \quad \frac{\gamma_{IR,3\ell}}{\gamma_{IR,3\ell,L}} = 0.913, \quad \frac{\gamma_{IR,4\ell}}{\gamma_{IR,4\ell,L}} = 0.880. \quad (6.16)$$

Performing the corresponding analysis for $N_c = 3$, $N_f = 15$, we obtain

$$\frac{\gamma_{IR,2\ell}}{\gamma_{IR,2\ell,L}} = 0.943, \quad \frac{\gamma_{IR,3\ell}}{\gamma_{IR,3\ell,L}} = 0.929, \quad \frac{\gamma_{IR,4\ell}}{\gamma_{IR,4\ell,L}} = 0.929. \quad (6.17)$$

These numerical comparisons show that even for a moderate value of N_c such as $N_c = 3$, the values of these IR zeros of $\beta_{\alpha,n,\ell}$ and anomalous dimensions $\gamma_{IR,n\ell}$ are close to the approximations that one obtains from the LNN limit. The agreement becomes better as N_c increases.

From our analysis, it follows that the approach to the LNN limit is of the same form for other structural properties describing the UV to IR evolution of the theory; that is, the first subleading correction term to the LNN limit is suppressed by $1/N_c^2$. We show this explicitly for additional two-loop quantities. The result for $\alpha_{m,2\ell}$ follows immediately from Eqs. (4.5), (4.6), and (6.8). For $(\beta_{IR,2\ell})_{min}$, the approach to the LNN limit has the form

$$(\beta_{IR,2\ell})_{min} N_c = (\beta_{\xi,2\ell})_{min} - \frac{2^6 \pi r (11 - 2r)^3}{3^3 (13r - 34)^3 N_c^2} + O\left(\frac{1}{N_c^4}\right), \quad (6.18)$$

where $(\beta_{\xi,2\ell})_{min}$ was given in Eq. (4.16). For the derivative of β at the n -loop IR zero of β , the approach to the LNN limit has the form

$$\left. \frac{d\beta_{\alpha,2\ell}}{d\alpha} \right|_{\alpha=\alpha_{IR,2\ell}} = \left. \frac{d\beta_{\xi,2\ell}}{d\xi} \right|_{\xi=\xi_{IR,2\ell}} + \frac{2r(11-2r)^2}{(13r-34)^2 N_c^2} + O\left(\frac{1}{N_c^4}\right), \quad (6.19)$$

where $d\beta_{\xi,2\ell}/d\xi|_{\xi=\xi_{IR,2\ell}} = \beta'_{\xi,IR,2\ell}$ was given in Eq. (4.20).

VII. CONTRAST WITH FERMIONS IN HIGHER REPRESENTATIONS

Gauge theories with fermions in higher-dimensional representations, in particular, two-index representations, are also of interest [28]. We comment briefly here on the adjoint, and symmetric and antisymmetric rank-2 tensor representations with Young tableaux $\square\square$ and $\square\square$. Rather than an LNN limit, in these cases, one takes N_f equal to a (non-negative, integer) constant as $N_c \rightarrow \infty$ to get a finite limit. For the adjoint representation, b_ℓ/N_c^ℓ is a constant for $\ell = 1, 2, 3$, while b_4/N_c^4 is equal to a constant plus a $1/N_c^2$ correction term (where b_ℓ with $\ell = 3, 4$ are calculated in the \overline{MS} scheme). For the S2 ($\square\square$) and A2 ($\square\square$) representations, symbolized together as T2, the corrections to the $N_c \rightarrow \infty$ limit go like $1/N_c$ instead of $1/N_c^2$. For example,

$$\frac{b_1}{N_c} = \frac{11 - 2N_f}{3} \mp \frac{2N_f}{N_c} \quad \text{for T2}, \quad (7.1)$$

where the upper (lower) sign applies to S2 (A2).

These differences are reflected in the large- N_c corrections to the n -loop expressions for the IR zero of β . We

illustrate this at the two-loop level. For the adjoint representation, $N_{f,b1z} = 11/4$ and $N_{f,b2z} = 17/16$, so that there is only a single integer value of N_f for which the theory is asymptotically free and has an IR zero in $\beta_{2\ell}$, namely $N_f = 2$. One has

$$\alpha_{IR,2\ell} N_c = \frac{2\pi(11 - 4N_f)}{16N_f - 17}, \quad R = adj \quad (7.2)$$

(independent of N_c) so the right-hand side is equal to $2\pi/5$ for the value $N_f = 2$, independent of N_c .

For the S2 and A2 representations (denoted T2 again), for large N_c ,

$$\alpha_{IR,2\ell} N_c = \frac{2\pi(11 - 2N_f)}{8N_f - 17} \pm \frac{6\pi N_f(-47 + 2N_f)}{(8N_f - 17)^2 N_c} + O\left(\frac{1}{N_c^2}\right) \quad \text{for } R = T2, \quad (7.3)$$

so that in these S2 and A2 cases, the leading correction to the $N_c \rightarrow \infty$ result goes like $1/N_c$.

VIII. SUPERSYMMETRIC GAUGE THEORY

A. $\beta_{\xi,s}$ Function and IR Zeros

Here we consider the LNN limit of an asymptotically free, vectorial gauge theory with $\mathcal{N} = 1$ supersymmetry, gauge group $G = \text{SU}(N_c)$, and a chiral superfield content Φ_i , $\tilde{\Phi}_i$, $i = 1, \dots, N_f$, in the \square , $\bar{\square}$ representations, respectively. One of the appeals of this theory is that a number of exact results on the infrared properties of the theory are known [29, 30], so one can compare perturbative predictions with these exact results. This was done for general G and various representations R , \bar{R} for the N_f pairs of chiral superfields Φ_i , $\tilde{\Phi}_i$ in [11, 12]. Our discussion of the LNN limit here extends the previous results in [11, 12] (see also [8, 31]).

The β function of this theory will be denoted $\beta_{\xi,s}$ and has the expansion (2.2) with \hat{b}_ℓ and \tilde{b}_ℓ replaced by $\hat{b}_{\ell,s}$ and $\tilde{b}_{\ell,s}$. Here and below we use the subscript s , standing for “supersymmetric”, to avoid confusion with the corresponding quantities discussed above in the nonsupersymmetric theory. Thus,

$$\hat{b}_{\ell,s} = \lim_{LNN} \frac{b_{\ell,s}}{N_c^\ell}, \quad \tilde{b}_{\ell,s} = \lim_{LNN} \frac{\bar{b}_{\ell,s}}{N_c^\ell}. \quad (8.1)$$

We denote the n -loop $\beta_{\xi,s}$ function as $\beta_{\xi,s,n\ell}$. The scheme-independent coefficients $b_{1,s}$ and $b_{2,s}$, were computed in [32] and [33], and $b_{3,s}$ was computed in [34] in the dimensional reduction (\overline{DR}) scheme [35].

In the LNN limit,

$$\hat{b}_{1,s} = 3 - r, \quad (8.2)$$

$$\hat{b}_{2,s} = 2(3 - 2r), \quad (8.3)$$

and, in the \overline{DR} scheme,

$$\hat{b}_{3,s} = 21 - 21r + 4r^2. \quad (8.4)$$

From these values of the coefficients of $\beta_{\xi,s}$, it follows that

$$r_{b1z,s} = 3 \quad (8.5)$$

and

$$r_{b2z,s} = \frac{3}{2}. \quad (8.6)$$

Asymptotic freedom requires $r < r_{b1z}$, and, in this range, the two-loop β function has an IR zero for $r > r_{b2z}$, so the interval $I_{r,s}$ is

$$I_{r,s} : \frac{3}{2} < r < 3. \quad (8.7)$$

This IR zero occurs at the value

$$\begin{aligned} \xi_{IR,2\ell,s} &= -\frac{\tilde{b}_{1,s}}{\tilde{b}_{2,s}} = -\frac{4\pi\hat{b}_{1,s}}{\hat{b}_{2,s}} \\ &= \frac{2\pi(3-r)}{2r-3}. \end{aligned} \quad (8.8)$$

The coefficient $\hat{b}_{3,s}$ vanishes at two values,

$$r_{b3z,s,(1,2)} = \frac{21 \pm \sqrt{105}}{8}. \quad (8.9)$$

Numerically, $r_{b3z,s,1} = 1.344$ and $r_{b3z,s,2} = 3.906$, so that

$$r_{b3z,s,1} < r_{b2z}, \quad r_{b3z,s,2} > r_{b1z}. \quad (8.10)$$

Since $b_{3,s} < 0$ for $r_{b3z,s,1} < r < r_{b3z,s,2}$, it follows that, in the \overline{DR} scheme,

$$\hat{b}_{3,s} < 0 \quad \forall \quad r \in I_r. \quad (8.11)$$

We list numerical values of the $\tilde{b}_{\ell,s}$ in Table VI.

The three-loop β function formally vanishes at two points away from the origin, at the zeros of $\tilde{b}_{1,s} + \tilde{b}_{2,s}\xi + \tilde{b}_{3,s}\xi^2$, namely

$$\xi = \frac{1}{2\tilde{b}_{3,s}} \left[-\tilde{b}_{2,s} \pm \sqrt{\tilde{b}_{2,s}^2 - 4\tilde{b}_{1,s}\tilde{b}_{3,s}} \right]. \quad (8.12)$$

By the same type of argument that was given above for the nonsupersymmetric theory, one may argue that the inequality (8.11) applies more generally than just in the \overline{DR} scheme. In the present context, this argument is that if the theory has an IR zero in the (scheme-independent) two-loop β function, it is reasonable to require that a scheme should preserve the existence of this IR zero at higher-loop level, this requires that $\tilde{b}_3 < 0 \quad \forall r \in I_{r,s}$. This follows since $\tilde{b}_{2,s} \rightarrow 0$ at the lower end of the interval $I_{r,s}$, so unless $\tilde{b}_{3,s} < 0$ in this interval, the quantity $\tilde{b}_{2,s}^2 - 4\tilde{b}_{1,s}\tilde{b}_{3,s}$ would become negative and the value of

the zeros of β at the three-loop level in Eq. (8.12) would be complex. Given that $\tilde{b}_3 < 0$ for $r \in I_{r,s}$, one may rewrite Eq. (8.12) in terms of positive quantities and pick out the relevant IR zero of $\beta_{\xi,s,3\ell}$ as

$$\xi_{IR,3\ell,s} = \frac{1}{2|\tilde{b}_{3,s}|} \left[-|\tilde{b}_{2,s}| + \sqrt{\tilde{b}_{2,s}^2 + 4\tilde{b}_{1,s}|\tilde{b}_{3,s}|} \right]. \quad (8.13)$$

Explicitly,

$$\xi_{IR,3\ell,s} = \frac{4\pi \left[-(2r-3) + \sqrt{C_s} \right]}{D_s} \quad (8.14)$$

where

$$C_s = -54 + 72r - 29r^2 + 4r^3 \quad (8.15)$$

and

$$D_s = -21 + 21r - 4r^2. \quad (8.16)$$

Note that $D_s > 0$ for $r_{b3z,s,1} < r < r_{b3z,s,2}$ and hence for all $r \in I_{r,s}$. Furthermore, C_s is positive-definite for $r \in I_{r,s}$ (the zeros of C_s occur at $r = 1.338$ and $r = 2.956 \pm 1.163i$). By the same reasoning as was given before in [12] and above, we have the inequality

$$\xi_{IR,3\ell,s} < \xi_{IR,2\ell,s}. \quad (8.17)$$

We list numerical values of $\xi_{IR,n\ell,s}$ in Table VII and show a plot of $\beta_{\xi,n\ell,s}$ for $n = 2$ and $n = 3$ loops, evaluated at an illustrative value r in $I_{r,s}$, namely, $r = 2.5$ in Fig. 2.

B. Other Structural Features of $\beta_{\xi,n\ell,s}$

We also briefly discuss some structural features of $\beta_{\xi,s}$. The two-loop β function, $\beta_{\xi,s,2\ell}$, reaches a minimum on the interval $I_{r,s}$ at the value

$$\xi_{m,2\ell,s} = \frac{4\pi(3-r)}{2r-3}. \quad (8.18)$$

The ratio of this position of the minimum in the beta function relative to the position of the IR zero is the same as in the nonsupersymmetric theory, namely

$$\frac{\xi_{m,2\ell,s}}{\xi_{IR,2\ell,s}} = \frac{2}{3}. \quad (8.19)$$

The value of $\beta_{\xi,2\ell,s}$ at the minimum is

$$(\beta_{\xi,2\ell,s})_{min} = -\frac{8\pi(3-r)^3}{27(2r-3)^2}. \quad (8.20)$$

The derivative $d\beta_{\xi,IR,2\ell,s}$ evaluated at $\xi = \xi_{IR,2\ell,s}$ is

$$\beta'_{\xi,IR,2\ell,s} = \frac{(3-r)^2}{2r-3}. \quad (8.21)$$

Corresponding expressions can be given at the three-loop level, but we proceed now to analyze a quantity of considerable interest, namely the anomalous dimension of $\Phi\tilde{\Phi}$.

C. Anomalous Dimension

We next consider the LNN limit of the anomalous dimension of the (gauge-invariant) quadratic chiral superfield product, $\Phi\tilde{\Phi}$, denoted $\gamma_s \equiv \gamma_{m,s}$. This is given by Eq. (5.1) with the replacements $\hat{c}_\ell \rightarrow \hat{c}_{\ell,s}$ and $\tilde{c}_\ell \rightarrow \tilde{c}_{\ell,s}$, and similarly for the n -loop expression, $\gamma_{m,s,n\ell}$. From the known results for $c_{1,s}$ and, in the \overline{DR} scheme, $c_{2,s}$ and $c_{3,s}$, we find, in the LNN limit,

$$\hat{c}_{1,s} = 2 \quad (8.22)$$

$$\hat{c}_{2,s} = 2(2-r) \quad (8.23)$$

and

$$\hat{c}_{3,s} = 10 - 6r[1 + 2\zeta(3)] - 2r^2. \quad (8.24)$$

Values of the corresponding $\tilde{c}_{\ell,s}$ are listed as a function of r in Table VIII.

The two-loop anomalous dimension, evaluated at the two-loop IR zero of $\beta_{\xi,s}$, is [11]

$$\gamma_{IR,2\ell,s} = \frac{r(r-1)(3-r)}{2(2r-3)^2}. \quad (8.25)$$

The quantity $\gamma_{IR,2\ell,s}$ is a monotonically decreasing function of r in the interval $I_{r,s}$. It exceeds the upper bound of 1 from conformal symmetry if $r < 2$, and hence, as was noted in [11], in the interval $3/2 < r < 2$, the perturbative two-loop calculation that yields $\gamma_{IR,2\ell,s}$ gives an unphysical result and is unreliable. One can apply this upper bound because one knows from exact results [30] that for $3/2 < r < 3$, the theory flows in the infrared to a conformal, non-Abelian Coulomb phase.

The three-loop anomalous dimension, evaluated at the three-loop IR zero of $\beta_{\xi,s}$, is

$$\gamma_{IR,3\ell,s} = \frac{2(A_s + B_s\sqrt{C_s})}{D_s^3}, \quad (8.26)$$

where C_s and D_s were defined above in Eqs. (8.15) and (8.16), and A_s and B_s are given in the appendix. In contrast to $\gamma_{IR,2\ell,s}$, $\gamma_{IR,3\ell,s}$ is not a monotonic function of r . It reaches a maximum of approximately 0.1376 at $r = 2.474$ and vanishes not just at $r = r_{b1z} = 3$, but also at $r = 2.1794$ (to the indicated number of significant figures). These features were evident for the specific values of N_c considered in [11]; here we have shown how this occurs after the LNN limit is taken. In Table IX we list values of $\gamma_{IR,n\ell,s}$ for a range of r values in $I_{r,s}$. We note that for $1.5 < r < 2.0$, $\gamma_{IR,2\ell,s}$ exceeds the upper bound of 1 and hence is unphysical; we do not include entries for these values of r .

IX. DISCUSSION AND CONCLUSIONS

In summary, we have studied higher-loop corrections to the UV to IR evolution of an asymptotically free vectorial $SU(N_c)$ gauge theory with N_f fermions in the fundamental representation, in the 't Hooft-Veneziano (LNN)

limit $N_c \rightarrow \infty$ and $N_f \rightarrow \infty$ with $r = N_f/N_c$ fixed and $\xi(\mu) = \alpha(\mu)N_c$, a function independent of N_c in this limit. We have defined a beta function, β_ξ , that is finite in this LNN limit and have analyzed its properties for the interval of r in which $\beta_{\xi,2\ell}$ has an IR zero. We have given analytic and numerical results for the LNN limiting quantities $\xi_{IR,n\ell}$, $\xi_{m,n\ell}$, $(\beta_{\xi,n\ell})_{min}$, $\beta'_{\xi,IR,n\ell}$, and $\gamma_{IR,n\ell}$ as functions of r . We have argued that a reasonable scheme should preserve at higher loops the IR zero that is present at the (scheme-independent) two-loop order in β , and that this implies that $\tilde{b}_3 < 0$ for $r \in I_r$. In turn, this implies that $\xi_{IR,3\ell} < \xi_{IR,2\ell}$. Calculating with the \overline{MS} scheme, we find that in the part of the interval I_r where the perturbative calculations are reliable, the change in the IR zero is smaller in magnitude going from three-loop to four-loop order, as compared with the shift from two-loop to three-loop order. This is in agreement with one's expectation, that insofar as perturbative methods are trustworthy, when a quantity is calculated to higher orders, the successive changes should become smaller. Further, we find that for the range of $r \in I_r$ where the three-loop anomalous dimension is reliably calculable, $\gamma_{IR,3\ell} < \gamma_{IR,2\ell}$. These higher-loop calculations allow one to extend the analysis of the IR zero of the β function, and corresponding evaluations of γ_m to smaller values of r and thus stronger couplings than is possible with the two-loop result. We have analyzed the correction terms to the LNN-limit values of a number of quantities, including b_ℓ/N_c^ℓ , c_ℓ/N_c^ℓ , $\alpha_{IR,n\ell}N_c$, $\alpha_{m,n\ell}N_c$, $(\beta_{\alpha,n\ell})_{min}N_c$, $d\beta_{\alpha,n\ell}/d\alpha|_{\alpha_{IR,n\ell}}$, and

$\gamma_{IR,n\ell}$, and have shown that these correction terms are suppressed by $1/N_c^2$. This provides an understanding of the approximate universality that is exhibited in calculations of these quantities for different values of N_c and N_f with similar or identical values of r , even for moderate values of N_c and N_f . A corresponding analysis was also given of a vectorial gauge theory with $\mathcal{N} = 1$ supersymmetry and N_f chiral superfields transforming according to the fundamental and conjugate fundamental representation of $SU(N_c)$. Thus, in addition to being of interest in its own right, the LNN limit is useful in understanding common features of the UV to IR evolution of various theories with different values of N_c and N_f .

Acknowledgments: I would like to thank T. Rytov for collaboration on the earlier works [9, 11, 25], and T. Appelquist and the theory group at Yale University for warm hospitality during the sabbatical period when some of this work was done. This research was partially supported by the grant NSF-PHY-09-69739.

X. APPENDIX

In this appendix we list some of the more lengthy expressions that are used in the text. The functions $F_{3\ell}$ and $G_{3\ell}$ that enter in Eq. (4.17) for $(\beta_{\xi,3\ell})_{min}$ are

$$F_{3\ell} = -10985980784 + 17408705952r - 10177907376r^2 + 2883132208r^3 - 468256107r^4 + 42131712r^5 - 1605632r^6 \quad (10.1)$$

and

$$G_{3\ell} = 41737992 - 48660252r + 18696078r^2 - 2733297r^3 + 139776r^4. \quad (10.2)$$

For the coefficient c_4 in Eq. (5.1) (with fermions in the fundamental representation, and in the \overline{MS} scheme), using [26], we find

$$\begin{aligned} c_4 = & \hat{c}_4 + \frac{1}{N_c^2} \left[-\frac{21947}{24} + \frac{126689}{324}r - \frac{1127}{162}r^2 + \frac{83}{81}r^3 + \left(-\frac{221}{9} + \frac{379}{3}r - \frac{16}{9}r^2 \right) \zeta(3) - 60r\zeta(5) \right] \\ & + \frac{1}{N_c^4} \left[\frac{108359}{288} - \frac{9143}{108}r + \frac{38}{27}r^2 + (-151 + 59r - 20r^2)\zeta(3) + r(-66 + 12r)\zeta(4) + (220 - 160r)\zeta(5) \right] \\ & + \frac{1}{N_c^6} \left[-\frac{5783}{24} - \frac{37}{3}r + (89 + 111r)\zeta(3) + 60r\zeta(5) \right] + \frac{1}{N_c^8} \left[-\frac{1261}{64} - 42\zeta(3) \right]. \end{aligned} \quad (10.3)$$

The functions A_s and B_s that enter in the expression for $\gamma_{IR,3\ell,s}$ are

$$A_s = 918 - 2916r + 4146r^2 - 3322r^3 + 1532r^4 - 378r^5 + 40r^6 + r(2754 - 5508r + 3942r^2 - 1212r^3 + 144r^4)\zeta(3) \quad (10.4)$$

and

$$B_s = 54 - 75r + 17r^2 + 7r^3 + 5r^4 - 4r^5 + r(162 - 216r + 102r^2 - 24r^3)\zeta(3). \quad (10.5)$$

-
- [1] C. G. Callan, Phys. Rev. D **2**, 1541 (1970); K. Symanzik, Commun. Math. Phys. **18**, 227 (1970). See also M. Gell-Mann and F. Low, Phys. Rev. **95**, 1300 (1954); N. N. Bogolubov and D. V. Shirkov, Doklad. Akad. Nauk SSSR **103**, 391 (1955); K. Wilson, Phys. Rev. D **3**, 1818 (1971).
- [2] Our restriction to massless fermions is only for technical convenience. It is easy to include fermion mass terms, which are gauge-invariant in a vectorial gauge theory. However, if a given fermion has a mass m , it is integrated out of the effective field theory applicable at scales $\mu < m$ and does not affect the evolution in this region.
- [3] D. J. Gross and F. Wilczek, Phys. Rev. Lett. **30**, 1343 (1973); H. D. Politzer, Phys. Rev. Lett. **30**, 1346 (1973); G. 't Hooft, unpublished.
- [4] W. E. Caswell, Phys. Rev. Lett. **33**, 244 (1974); D. R. T. Jones, Nucl. Phys. B **75**, 531 (1974).
- [5] T. Banks and A. Zaks, Nucl. Phys. B **196**, 189 (1982).
- [6] O. V. Tarasov, A. A. Vladimirov, and A. Yu. Zharkov, Phys. Lett. B **93**, 429 (1980); S. A. Larin and J. A. M. Vermaseren, Phys. Lett. B **303**, 334 (1993).
- [7] T. van Ritbergen, J. A. M. Vermaseren, and S. A. Larin, Phys. Lett. B **400**, 379 (1997).
- [8] E. Gardi and M. Karliner, Nucl. Phys. B **529**, 383 (1998); E. Gardi and G. Grunberg, JHEP **03**, 024 (1999).
- [9] T. A. Ryttov and R. Shrock, Phys. Rev. D **83**, 056011 (2011), arXiv:1011.4542.
- [10] C. Pica and R. Sannino, Phys. Rev. D **83**, 035013 (2011), arXiv:1011.5917.
- [11] T. A. Ryttov, R. Shrock, Phys. Rev. D **85**, 076009 (2012), arXiv:1202.1297.
- [12] R. Shrock, arXiv:1301.3209.
- [13] G. 't Hooft, Nucl. Phys. B **72**, 461 (1974), Nucl. Phys. B **75**, 461 (1974).
- [14] G. Veneziano, Nucl. Phys. B **117**, 519 (1976).
- [15] C.-K. Chow and T.-M. Yan, Phys. Rev. D **53**, 5105 (1996); R. Shrock, Phys. Rev. D **53**, 6465 (1996); R. Shrock, Phys. Rev. D **76**, 055010 (2007).
- [16] H. E. Stanley, Phys. Rev. **176**, 718 (1968); Phys. Rev. **179**, 570 (1969).
- [17] Some early applications of the large- N limit to quantum field theories include H. J. Schnitzer, Phys. Rev. D **10**, 1800 (1974); S. R. Coleman, R. Jackiw, and H. D. Politzer, Phys. Rev. D **10**, 2491 (1974); D. J. Gross and A. Neveu, Phys. Rev. D **10**, 3235 (1974); C. G. Callan, N. Coote, and D. G. Gross, Phys. Rev. D **13**, 1649 (1976); E. Brézin and J. Zinn-Justin, Phys. Rev. B **14**, 3110 (1976); W. A. Bardeen, B. W. Lee, and R. E. Shrock, Phys. Rev. D **14**, 985 (1976); M. B. Einhorn, S. Nussinov, and E. Rabinovici, Phys. Rev. D **15**, 2282 (1977); J. Koplik, A. Neveu, S. Nussinov, Nucl. Phys. B **123**, 109 (1977); R. C. Brower, J. Ellis, M. G. Schmidt, and J. H. Weis, Nucl. Phys. **128**, 131 (1977); B. De Wit and G. 't Hooft, Phys. Lett. B **69**, 61 (1977); T. T. Wu, Phys. Lett. B **71**, 142 (1977); E. Brézin, C. Itzykson, G. Parisi, and J.-B. Zuber, Commun. Math. Phys. **59**, 35 (1978); E. Witten, Nucl. Phys. B **160**, 57 (1979); E. Corrigan and P. Ramond, Phys. Lett. B **87**, 73 (1979); Yu. Makeenko and A.A. Migdal, Phys. Lett. B **88**, 135 (1979); S. R. Coleman and E. Witten, Phys. Rev. Lett. **45**, 100 (1980); H. Neuberger, Phys. Lett. B **94**, 199 (1980).
- [18] For a recent review with references to the extensive literature on large- N methods, see B. Lucini and M. Panero, Phys. Repts., in press (2013).
- [19] The Casimir invariants C_R and T_R are defined as $\sum_a \sum_j \mathcal{D}_R(T_a)_{ij} \mathcal{D}_R(T_a)_{jk} = C_R \delta_{ik}$ and $\sum_{i,j} \mathcal{D}_R(T_a)_{ij} \mathcal{D}_R(T_b)_{ji} = T_R \delta_{ab}$, where R is the representation and T_a are the generators of G , so that for $SU(N_c)$, $C_A = N_c$ for the adjoint (A) and $T_{fund} = 1/2$ for the fundamental representation, etc. C_f denotes C_R for the fermion representation.
- [20] T. Appelquist, J. Terning, and L. C. R. Wijewardhana, Phys. Rev. Lett. **77**, 1214 (1996).
- [21] See [9, 12] for further references on this. For recent reviews of lattice and continuum studies of this chiral transition for various N_c , fermion representations, and N_f , see, e.g., the talks at the conferences *Lattice Meets Experiment 2012: Beyond the Standard Model*, Univ. of Colorado, Oct., 2012, URL <http://www-hep.colorado.edu/~schaich/lat-exp-2012> and *Proceedings of Strongly Coupled Gauge Theories in the LHC Perspective*, Dec., 2012, Univ. of Nagoya, ed. K. Yamawaki, to appear.
- [22] G. 't Hooft, Nucl. Phys. B **61**, 455 (1973).
- [23] W. A. Bardeen, A. J. Buras, D. W. Duke, and T. Muta, Phys. Rev. D **18**, 3998 (1978).
- [24] S. Bethke, Eur. Phys. J. C **64**, 689 (2009).
- [25] T. A. Ryttov and R. Shrock, Phys. Rev. D **86**, 065032 (2012), arXiv:1206.2366; Phys. Rev. D **86**, 085005 (2012), arXiv:1206.6895.
- [26] J. A. M. Vermaseren, S. A. Larin, and T. van Ritbergen, Phys. Lett. B **405**, 327 (1997).
- [27] S. Ferrara, R. Gatto, A. F. Grillo, Phys. Rev. D **9**, 3564 (1974); G. Mack, Commun. Math. Phys. **55**, 1 (1977); B. Grinstein, K. Intriligator, and I. Rothstein, Phys. Lett. B **662**, 367 (2008).
- [28] A recent review is F. Sannino, Acta Phys. Polon. B **40**, 3533 (2009).
- [29] V. A. Novikov, M. A. Shifman, A. I. Vainshtein, and V. I. Zakharov, Nucl. Phys. B **229**, 381 (1983); Nucl. Phys. B **277**, 426 (1986).
- [30] N. Seiberg, Phys. Rev. D **49**, 6857 (1994); Nucl. Phys. B **435**, 129 (1995); K. A. Intriligator and N. Seiberg, Nucl. Phys. B **444**, 125 (1995).
- [31] R. Oehme, Phys. Lett. B **399**, 67 (1997); M. T. Frandsen, T. Pickup, and M. Teper, Phys. Lett. B **695**, 231 (2011).
- [32] D. R. T. Jones, Nucl. Phys. B **87**, 127 (1975).
- [33] M. Machacek and M. Vaughn, Nucl. Phys. B **222**, 83 (1983); A. J. Parkes and P. C. West, Phys. Lett. B **138**, 99 (1984); Nucl. Phys. B **256**, 340 (1985); D. R. T. Jones and L. Mezincescu, Phys. Lett. B **136**, 242 (1984); Phys. Lett. B **138**, 293 (1984).
- [34] R. V. Harlander, D. R. T. Jones, P. Kant, L. Mihaila, and M. Steinhauser, JHEP **0612**, 024 (2006); R. Harlander, L. Mihaila, and M. Steinhauser, Eur. Phys. J. C **63**, 383 (2009).
- [35] W. Siegel, Phys. Lett. B **84**, 193 (1979); Phys. Lett. B **94**, 37 (1980); a recent discussion is W. Stöckinger, JHEP **0503**, 076 (2005).

TABLE I: Values of the \tilde{b}_ℓ coefficients for $1 \leq \ell \leq 4$ as functions of r for $0 \leq r \leq r_{b1z}$. Notation $ae-n$ means $a \times 10^{-n}$ here and in the other tables.

r	\tilde{b}_1	\tilde{b}_2	\tilde{b}_3	\tilde{b}_4
0.0	0.2918	0.7177e-1	0.2666e-1	0.1265e-1
0.5	0.2653	0.5805e-1	0.1895e-1	0.8063e-2
1.0	0.2387	0.4433e-1	0.1176e-1	0.4429e-2
1.5	0.2122	0.3061e-1	0.5091e-2	0.1766e-2
2.0	0.1857	0.1689e-1	-0.1055e-2	0.9062e-4
2.5	0.1592	0.3166e-2	-0.6677e-2	-0.5814e-3
3.0	0.1326	-0.1055e-1	-0.1178e-1	-0.2340e-3
3.5	0.1061	-0.2427e-1	-0.1635e-1	0.1149e-2
4.0	0.7958e-1	-0.3800e-1	-0.2041e-1	0.3584e-2
4.5	0.5305e-1	-0.5172e-1	-0.2394e-1	0.7086e-2
5.0	0.2653e-1	-0.6544e-1	-0.2695e-1	0.1167e-1
5.5	0	-0.7916e-1	-0.2944e-1	0.1736e-1

TABLE II: Values of the \tilde{b}_ℓ with $1 \leq \ell \leq 4$ at special values of r , including $r = 0$ and at the lower and upper ends of the interval I_r , $r = r_{b2z} = 34/13$, and $r = r_{b1z} = 11/2$.

ℓ	$(\tilde{b}_\ell)_{r=0}$	$(\tilde{b}_\ell)_{r=r_{b2z}}$	$(\tilde{b}_\ell)_{r=r_{b1z}}$
1	0.2918	0.1530	0
2	0.7177e-1	0	-0.7916e-1
3	0.2666e-1	-0.7900e-2	-0.2944e-2
4	0.1265e-1	-0.5923e-3	0.1736e-1

TABLE III: Values of the IR zero $\xi_{IR,n\ell}$ of $\beta_{\xi,n\ell}$ function for $n = 2, 3, 4$ and $r \in I_r$.

r	$\xi_{IR,2\ell}$	$\xi_{IR,3\ell}$	$\xi_{IR,4\ell}$
2.8	28.274	3.573	3.323
3.0	12.566	2.938	2.868
3.2	7.606	2.458	2.494
3.4	5.174	2.076	2.168
3.6	3.731	1.759	1.873
3.8	2.774	1.489	1.601
4.0	2.095	1.252	1.349
4.2	1.586	1.041	1.115
4.4	1.192	0.8490	0.9003
4.6	0.8767	0.6725	0.7038
4.8	0.6195	0.5083	0.5244
5.0	0.4054	0.3538	0.3603
5.2	0.2244	0.2074	0.2089
5.4	0.06943	0.06769	0.06775

TABLE IV: Values of the \tilde{c}_ℓ coefficients with $1 \leq \ell \leq 4$ as functions of r for $0 \leq r \leq r_{b1z}$. Here $\tilde{c}_1 = 3/(4\pi) = 0.2387$, independent of r .

r	\tilde{c}_2	\tilde{c}_3	\tilde{c}_4
0.0	0.1071	0.5325e-1	0.2908e-1
0.5	0.1018	0.4396e-1	0.2098e-1
1.0	0.9657e-1	0.3434e-1	0.1324e-1
1.5	0.9129e-1	0.2440e-1	0.5897e-2
2.0	0.8602e-1	0.1413e-1	-0.1010e-2
2.5	0.8074e-1	0.3538e-2	-0.7451e-2
3.0	0.7546e-1	-0.7384e-2	-0.1339e-1
3.5	0.7019e-1	-0.1863e-1	-0.1880e-1
4.0	0.6491e-1	-0.3021e-1	-0.2364e-1
4.5	0.5963e-1	-0.4211e-1	-0.2788e-1
5.0	0.5435e-1	-0.5434e-1	-0.3148e-1
5.5	0.4908e-1	-0.6690e-1	-0.3442e-1

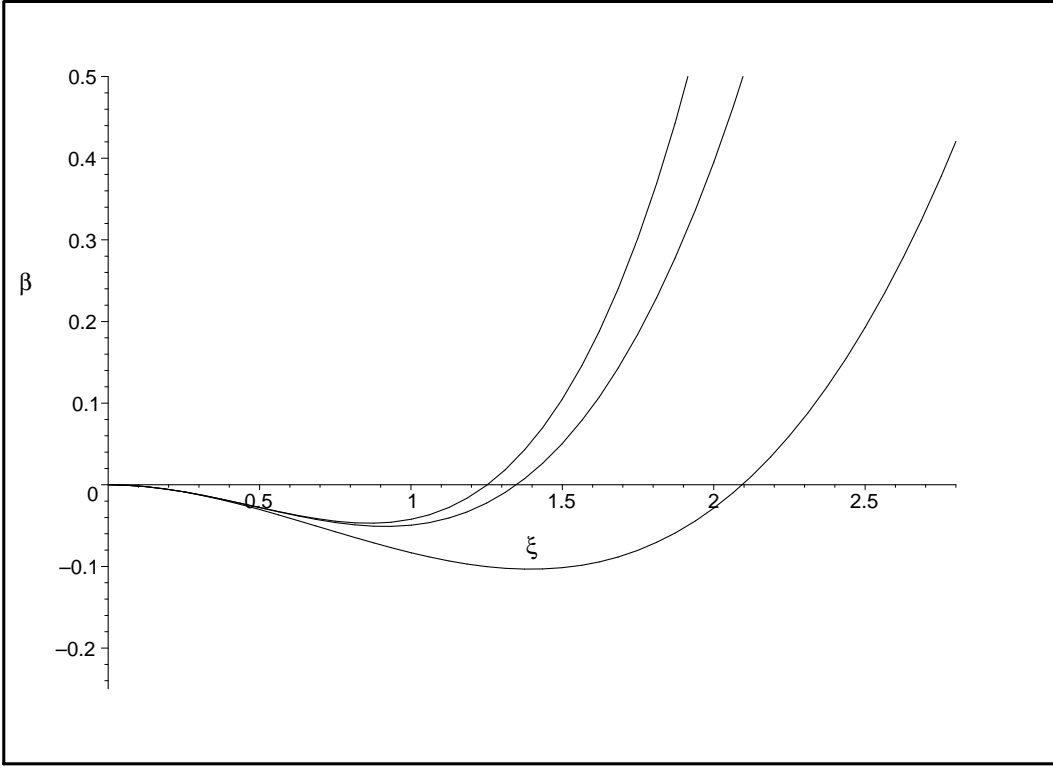


FIG. 1: Plot of the n -loop beta function, $\beta_{\xi,n\ell}$, as a function of ξ , for the illustrative value $r = 4$. From bottom to top, the curves represent $\beta_{\xi,2\ell}$, $\beta_{\xi,4\ell}$, and $\beta_{\xi,3\ell}$, respectively.

TABLE V: Values of the n -loop anomalous dimension, $\gamma_{n\ell}$, evaluated at the n -loop IR zero of β_ξ and denoted $\gamma_{IR,n\ell}$, as in Eq. (5.12), where $n = 2, 3, 4$, for $r \in I_r$. In the entries marked u, the n -loop perturbative value of $\gamma_{IR,n\ell}$ is larger than the upper bound of 2 and hence is unphysical (u).

r	$\gamma_{IR,2\ell}$	$\gamma_{IR,3\ell}$	$\gamma_{IR,4\ell}$
2.8	u	1.708	0.1902
3.0	u	1.165	0.2254
3.2	u	0.8540	0.2637
3.4	u	0.6563	0.2933
3.6	1.853	0.5201	0.3083
3.8	1.178	0.4197	0.3061
4.0	0.7847	0.3414	0.2877
4.2	0.5366	0.2771	0.2664
4.4	0.3707	0.2221	0.2173
4.6	0.2543	0.1735	0.1745
4.8	0.1696	0.1294	0.1313
5.0	0.1057	0.08886	0.08999
5.2	0.05620	0.05123	0.05156
5.4	0.01682	0.01637	0.01638

TABLE VI: Values of the $\tilde{b}_{\ell,s}$ coefficients for $1 \leq \ell \leq 3$ as functions of r for $0 \leq r \leq r_{b1z,s}$ in the supersymmetric theory.

r	$\tilde{b}_{1,s}$	$\tilde{b}_{2,s}$	$\tilde{b}_{3,s}$
0.0	0.2387	0.3800e-1	0.1058e-1
0.5	0.1989	0.2533e-1	0.5795e-2
1.0	0.1592	0.1267e-1	0.20166e-2
1.5	0.1194	0	-0.7559e-3
2.0	0.7958e-1	-0.1267e-1	-0.2520e-2
2.5	0.3979e-1	-0.2533e-1	-0.3276e-2
3.0	0	-0.3800e-1	-0.3024e-2

TABLE VII: Values of the IR zero $\xi_{IR,n\ell,s}$ of $\beta_{\xi,n\ell,s}$ function for $n = 2$ and $n = 3$ loops and $r \in I_{r,s}$.

r	$\xi_{IR,2\ell,s}$	$\xi_{IR,3\ell,s}$
1.8	12.566	5.331
1.9	8.639	4.381
2.0	6.283	3.643
2.1	4.712	3.040
2.2	3.590	2.529
2.3	2.749	2.085
2.4	2.094	1.692
2.5	1.571	1.339
2.6	1.142	1.019
2.7	0.7854	0.7279
2.8	0.4833	0.4623
2.9	0.2244	0.2201

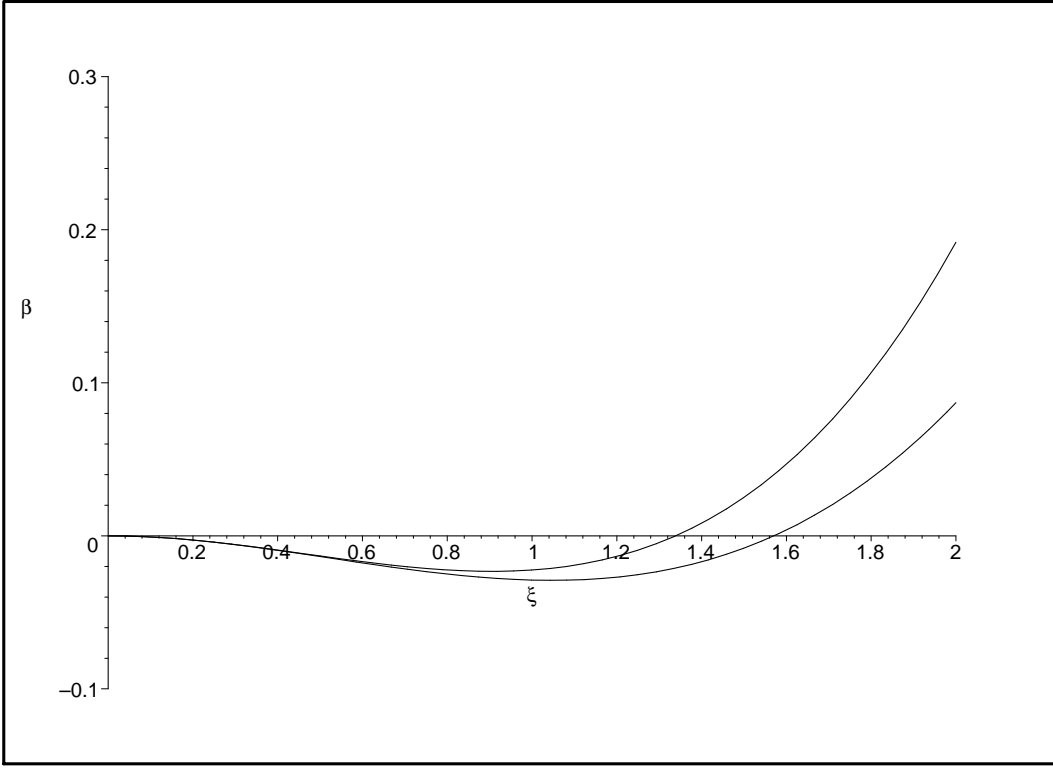


FIG. 2: Plot of the n -loop beta function, $\beta_{\xi, n\ell, s}$, as a function of ξ , for the illustrative value $r = 2.5$ in the supersymmetric theory. From bottom to top, the curves represent $\beta_{\xi, 2\ell, s}$ and $\beta_{\xi, 3\ell, s}$, respectively.

TABLE VIII: Values of the $\tilde{c}_{\ell, s}$ coefficients for $\ell = 2$ and $\ell = 3$, as functions of r for $0 \leq r \leq r_{b1z, s}$ in the supersymmetric theory. Here $\tilde{c}_{1, s} = 1/(2\pi) = 0.1592$, independent of r .

r	$\tilde{c}_{2, s}$	$\tilde{c}_{3, s}$
0.0	0.2533e-1	0.5039e-2
0.5	0.1900e-1	-0.3590e-3
1.0	0.1267e-1	-0.6261e-2
1.5	0.6333e-2	-0.1267e-1
2.0	0	-0.1958e-1
2.5	-0.6333e-2	-0.2699e-1
3.0	-0.1267e-1	-0.3491e-1

TABLE IX: Values of the n -loop anomalous dimension, $\gamma_{n\ell,s}$, evaluated at the n -loop IR zero of $\beta_{\xi,s}$ and denoted $\gamma_{IR,n\ell,s}$, where $n = 2$ and $n = 3$, for $r \in I_{r,s}$. For $1.5 < r < 2.0$, $\gamma_{IR,2\ell,s} > 1$ and hence is unphysical (u).

r	$\gamma_{IR,2\ell,s}$	$\gamma_{IR,3\ell,s}$
1.8	u	-1.617
1.9	u	-0.8053
2.0	1	-0.3667
2.1	0.7219	-1183
2.2	0.5388	0.2267e-1
2.3	0.4088	0.9809e-1
2.4	0.3111	0.1314
2.6	0.2344	0.1370
2.7	0.1719	0.9955e-1
2.8	0.7456e-1	0.6829e-1
2.9	0.3514e-1	0.3412e-1